Exploration of homogeneous ethylene dimerization mediated by tungsten mono(imido) complexes

Antonis M. Messinis,[†,§] William R. H. Wright,[†,§] Andrei S. Batsanov,[§] Judith A. K. Howard,[§] Martin J. Hanton,[,‡,¶] and Philip W. Dyer*[,†,§]*

[†]Centre for Sustainable Chemical Processes, Department of Chemistry, Durham University, South Road, Durham DH1 3LE, U.K.

[§]Department of Chemistry, Durham University, South Road, Durham, DH1 3LE, U.K.

[‡]Sasol UK Ltd, Purdie Building, North Haugh, St. Andrews, Fife, KY16 9ST, U.K.

[¶]Current address: TÜV SÜD NEL, East Kilbride, Glasgow, G75 0QF, U.K.

ABSTRACT

In combination with $EtAlCl_2$, complexes $[\{WCl_3(\mu\text{-}Cl)(N\text{-}2,6\text{-}i\text{Pr}_2C_6H_3)\}_2]$, $[WCl_4(NR)(thf)]$ (R=Et, *i*Pr, *c*Hx, Ph, 2,6-$i\text{Pr}_2C_6H_3$, 4-F-C_6H_4, 2,4,6-F_3-C_6H_2), and $[WCl_2(NR')(PMe_3)_3]$ (R'= Ph, 2,6-$i\text{Pr}_2C_6H_3$) were all productive ethylene dimerization pre-catalysts giving TONs in the range 400-144,000 (mol C_2H_4)(mol W)$^{-1}$ and moderate selectivities towards 1-butene (>66%) depending on the nature of the imido substituent. The formation of C_6 side products resulted from incorporation of 1-butene, rather than direct trimerization, something that is independent of butene

concentration. Stoichiometric reactions between the tungsten mono(imido) complexes and alkylaluminum reagents are described, which are consistent with reduction of the tungsten center playing an important part of the initiation process. Testing discrete W^{V} and W^{IV} mono(imido) complexes for olefin dimerization revealed the former to be significantly more active, which offers insight into the mode of action of the commercially relevant tungsten mono(imido) selective dimerization initiators described herein.

KEYWORDS: dimerization, ethylene, 1-butene, catalysis, tungsten, imido

TOC GRAPHIC

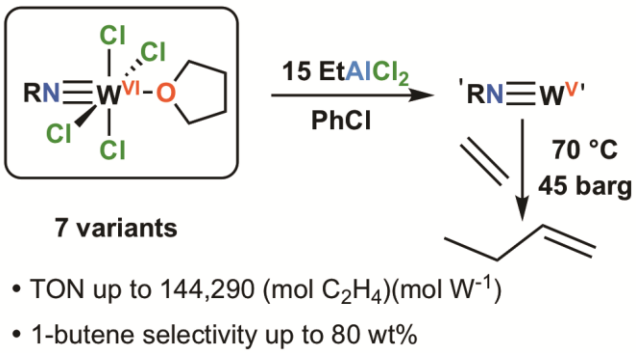

INTRODUCTION

Alkene oligomerization is a key industrial methodology for refinery product stream modification and for the preparation of versatile commodity chemical feed-stocks, in particular linear α-olefins (LAOs).[1-4] The importance of this area as a whole is reflected by a total annual production of ~5 million metric tons of LAOs, a market with an estimated worth of USD 14 billion in 2014.[5] In this arena a key raw material is 1-butene, which has a market value of ~USD 3.5 billion.[6] Demand for 1-butene arises from its use as a principal co-monomer for the manufacture of high density polyethylene (HDPE) and linear low-density polyethylene (LLDPE).[7-8] Additionally, 1-butene is the primary feed for the manufacture of methyl ethyl ketone and valeraldehyde, *via* hydroformylation, the latter finding wide application in the production of *n*-pentanol and valeric acid (intermediates used extensively in the manufacture of flavors and perfumes, synthetic lubricants, agrochemicals, and pharmaceuticals).[9]

Traditionally, 1-butene has been sourced from refinery streams, but today's market demand is fast outstripping supply, making development of alternative sources vital.[6] In this context catalytic ethylene dimerization has received particular attention offering a straightforward and economic method for the 'on-demand' manufacture of 1-butene, with a variety of well-defined early and late transition metal catalytic systems having been described,[10-22] including Axens' established Ti-based AlphaButol process.[23,24]

Controlling product selectivity remains an important challenge in butene manufacture since high purity 1-butene is required for co-monomer applications;[6] the economics of the process dictate efficient use of the ethylene feedstock; and to avoid formation of higher molecular weight

byproducts that lead to reactor fouling.[25] Consequently, the search for catalysts with enhanced performance continues, leading to renewed interest in a poorly defined system developed by Goodyear comprising tungsten hexachloride, a primary aniline, and an alkylaluminum co-initiator (e.g. $Et_3Al_2Cl_2$).[26-33] The resulting catalyst generated in situ mediates dimerization of both ethylene and short chain α-olefins with high selectivities, but is inconvenient and costly to prepare, as efficient removal of HCl is essential for optimal catalytic performance.[28,30,32-34] However, it has been demonstrated that both increased selectivity for dimerization (typically ≥99%) and extremely high selectivity to mono-methyl branching with α-olefin substrates can be achieved on addition of a tertiary amine base, e.g. NEt_3, prior to activation with an appropriate alkylaluminum chloride ($W:ArNH_2:NEt_3:Al$ = 1:2:2:10).[35,36] Thus, these dimerization systems offer scope for tuning product distributions, with not only the nature of the aniline, but also the identity of the alkylaluminum reagent and solvent having been shown to impact significantly on catalytic activity and selectivity.[35-36]

While the exact nature of the actual catalytically-active species in these WCl_6-derived catalysts is unknown, it has been proposed that tungsten aryl imido (ArN^{2-}) species are implicated.[24,37] This is supported by reports that, in combination with an appropriate alkylaluminum reagent,[35-37] discrete or immobilized imido complexes of the type $[WCl_4(NAr)]$ are active for ethylene and propylene dimerization, with related tungsten bis(imido) pre-catalysts $[WCl_2(NAr)_2]$ also exhibiting selective ethylene dimerization behavior.[24,37,38] In an extension to these studies, O'Hare and co-workers have recently described selective ethylene oligomerization mediated by discrete tungsten mono(imido) complexes immobilized on solid polymethylaluminoxane.[39]

Computational investigations of both mono- and bis-(imido) tungsten systems propose that the high selectivity to dimerization products is likely to result from a metallacyclic pathway involving

oxidative ethylene coupling, with termination to produce the α-olefin occurring via a combined β-hydride/reductive elimination pathway.[40-42] For the mono(imido) derivatives coordination of the alkylaluminum chloride to the tungsten chloro moiety (**A**, Figure 1) is pivotal in accessing the catalytically active reaction manifold, with the alternative arrangement in which the aluminum is bound *via* the imido nitrogen, **B**, being energetically inaccessible. In contrast, for the analogous bis(imido) systems, the formation of a WNAlCl metallacycle **C** is proposed in silico although in vitro observation of such group 6 metallacycles is rare.[37, 40, 43]

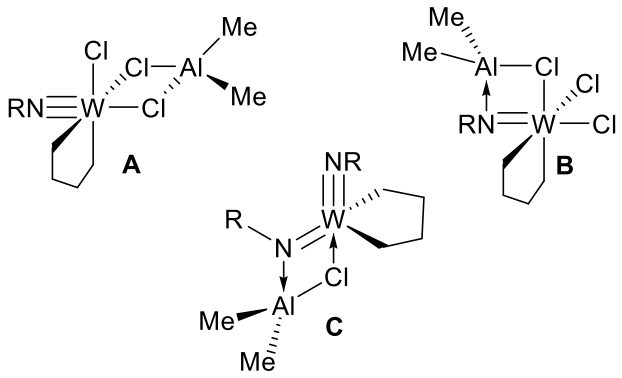

Figure 1. Computed modes of Me_2AlCl coordination to metallacyclopentane imido W^{VI} complexes of relevance to ethylene dimerization catalysis.[40]

To gain further insight into both the dimerization mechanism and the nature of the catalytically active species operative for $WCl_6/RNH_2/NEt_3/R'AlCl_2$ systems, we present here a study of the reactivity of discrete mono(imido) tungsten chloro complexes, $[WCl_4(NR)(THF)]$ and $[\{WCl_3(\mu\text{-}Cl)(NR)\}_2]$, towards alkylaluminum reagents, and the performance of these pre-catalysts in catalytic ethylene dimerization. These studies present an industrially relevant tungsten-based ethylene dimerization system and reveal information about the likely oxidation state of the active catalyst.

RESULTS AND DISCUSSION

To explore the viability of well-defined mono(imido) pre-catalysts in ethylene dimerization and to interrogate the effect of the nature of the imido substituent, a series of complexes was prepared in which the steric and electronic demands of the imido moiety was varied. Additionally, to probe the role of tungsten oxidation state in dimerization catalysis, a comparative study of W^{VI}, W^{V}, and W^{IV} systems was undertaken.

1. Complex Synthesis and Characterization. Both previously reported and new W^{VI} mono(imido) complexes $[WCl_4(NR)(thf)]$ (**2a**-**g**), were synthesized using modifications of literature procedures, whereby $WOCl_4$[44] was reacted with the appropriate organic isocyanate at reflux, leading to the formation of the chloride-bridged dimeric mono(imido) complexes $[\{WCl_3(\mu\text{-}Cl)(NR)\}_2]$ (**1a**-**g**) (Scheme 1).[38,45-51] The resulting dimers can be transformed into monometallic complexes **2** on treatment with excess THF. In contrast to complexes **1a**-**e**,**g**, the trifluorophenyl imido derivative **1f** mediates ring-opening of neat THF and hence was converted to its monometallic derivate **2f** by treatment with a stoichiometric quantity of THF in CH_2Cl_2 solution. This particular reactivity has been attributed to the enhanced Lewis acidity of the tungsten center of **1f**, which arises from the presence of the highly fluorinated, electron deficient imido moiety (vide infra).

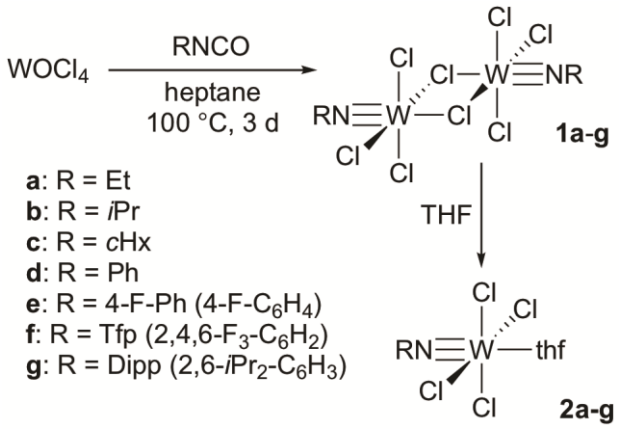

Scheme 1. Synthesis of complexes [{WCl_3(μ-Cl)(NR)}$_2$] (**1a-g**) and [WCl_4(NR)(thf)] (**2a-g**).[38,45-51]

For comparative purposes, the W^V mono(imido) complex [{WCl_2(NDipp)}$_2$(μ-Cl)$_3$][Et_4N] (**3**) was prepared using a modification of the synthetic methodology reported by Bradley and co-workers for the synthesis of [{WCl_2(NPh)}$_2$(μ-Cl)$_3$][$P(CH_2Ph)Ph_3$].[51] Thus, reaction of [WCl_4(NDipp)(thf)] with Et_4NCl in CH_2Cl_2 over sodium mercury amalgam, afforded complex **3** in 76 % yield (Scheme 2).

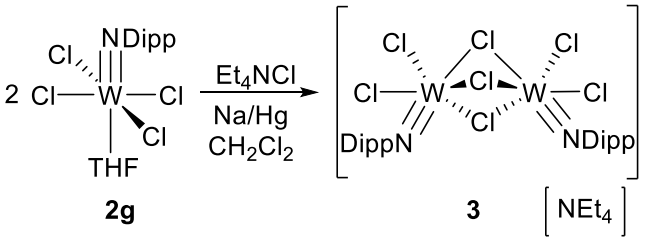

Scheme 2. Synthesis of [{WCl_2(NDipp)}$_2$(μ-Cl)$_3$][Et_4N] (**3**).

Complexes [WCl_2(NR)(PMe_3)$_3$] {R = Ph (**4a**) and Dipp (**4b**)} were synthesized according to slight modifications of literature procedures, by reacting complexes **2d** and **2g**, respectively, with sodium mercury amalgam (0.3%) in the presence of PMe_3 (Scheme 3).[52] The hydride complex

[WCl(H)(NDipp)(PMe_3)$_3$] (**5**) was prepared in moderate yield (55%) using an alteration of the synthesis described for the analogous molybdenum derivative, namely reaction of complex **4b** with L-selectride (lithium *tri-sec*-butyl(hydrido)borate) at –30 °C in toluene, Scheme 3.[53]

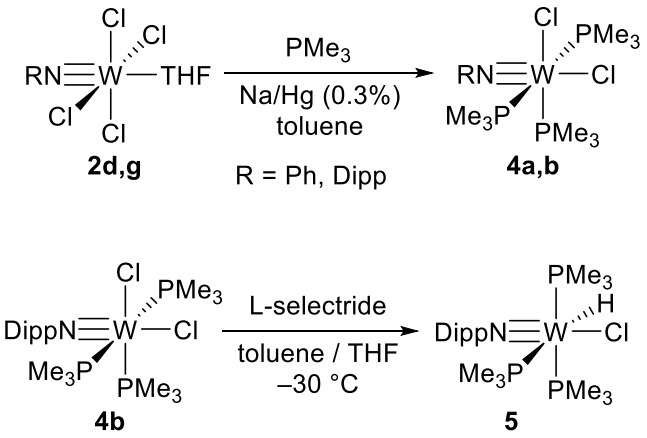

Scheme 3. Synthesis of complexes [WCl_2(NR)(PMe_3)$_3$] {R = Ph (**4a**) and Dipp (**4b**)} and [WCl(H)(NDipp)(PMe_3)$_3$] (**5**).

1.1 Molecular structure determinations. Structures of complexes **1f** and **1g** were established by single-crystal X-ray diffraction. Complex **1f** crystallized from toluene as **1f**·2 PhMe, featuring a well-established pattern of infinite stacks of alternating arene and trifluoroarene rings with an interplanar angle of 2.8° and mean separation of 3.39 Å (Table 1, Figure 2).[54,55]

Table 1. Selected bond distances (Å) and angles (°) in complexes **1** and **2**

Bond	**1a** [a]	**1f**·PhMe	**1g**	**1g**·C_6D_6	**2f**	**2g** [b]
W-Cl(1)	2.4391(11)	2.2929(7)	2.4168(9)	2.4317(8)	2.3309(5)	2.3320(7)
W-Cl(1')	2.7155(11)	--	2.7119(7)	2.7078(8)	--	--
W-Cl(2)	2.3062(12)	2.2701(8)	2.3163(8)	2.2983(8)	2.3286(6)	2.3287(7)
W-Cl(3)	2.2837(12)	2.3290(7)	2.2858(10)	2.2965(8)	2.3279(5)	2.3444(7)

W-Cl(4)	2.3167(12)	2.4381(8)	2.3175(8)	2.3152(8)	2.3309(5)	2.339(1)
W-Cl(4')	--	2.6725(6)	--	--	--	--
W-N	1.700(4)	1.727(2)	1.727(3)	1.722(3)	1.7227(19)	1.729(2)
N-C(1)	1.432(6)	1.361(3)	1.390(4)	1.392(4)	1.368(3)	1.386(3)
W-O	--	--	--	--	2.2363(15)	2.249(2)
W-N-C(1)	173.9(4)	173.7(2)	178.6(2)	178.9(3)	176.77(16)	178.1(2)

[a] Crystals of **1a** obtained in this work were examined by X-ray diffraction (see SI) with the structure being essentially the same as that determined previously.[45] [b] The asymmetric unit of **2g** contains two independent molecules with similar coordination geometry. Here, the average metric parameters are listed.

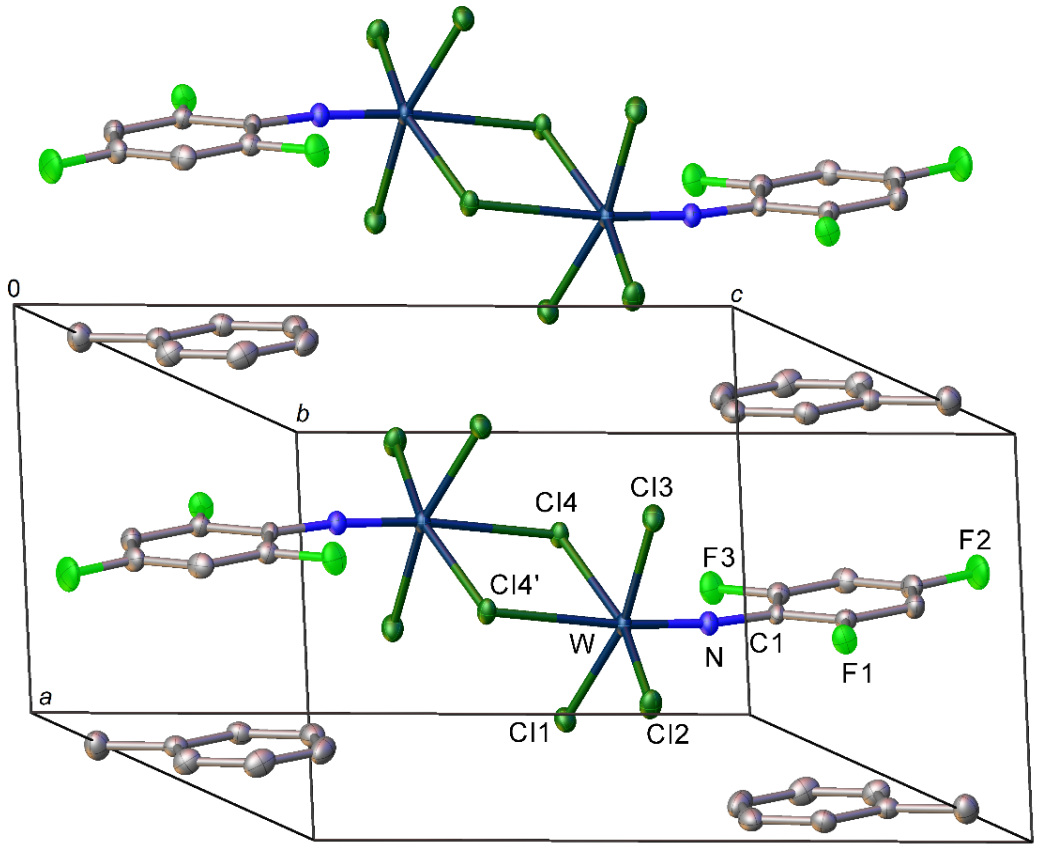

Figure 2. X-ray crystal structure of [{WCl_3(μ-Cl)(NTfp)}$_2$]·2 PhMe (**1f**) showing arene-fluoroarene π-π stacking. Thermal ellipsoids are drawn at the 50% probability level. Primed atoms are related by an inversion center.

Complex **1g** crystallized from CH_2Cl_2 in a solvent-free form and from deuterobenzene as **1g**·C_6D_6, without any significant change in the host molecule geometry (Table 1, Figure 3). In each case, **1g** has crystallographic C_i symmetry with the tungsten atoms having octahedral coordination and being linked by a pair of chloride bridges, which are asymmetric due to the strong *trans* effect[56] of the imido ligand, which acts as a LX_2 donor, i.e. presenting a *pseudo*-triple W≡NR bond.[57,58] The imido ligands of each complex have the same near-linear W-N-C arrangement (Table 1) and a typical imido W–N bond distance,[45,59,60] which is slightly shorter in the alkyl imido complex **1a**, due to the absence of π-conjugation with the aryl substituent. The asymmetry of the W-Cl-W bridge can be described as a displacement of the W atom from the equatorial Cl_4 plane towards the imido ligand, by ~0.30 Å. This can be regarded as a measure of the imido *trans* effect and is smaller in complex **1f** than in **1g**. However, this difference is minimal, being of the same order of magnitude as the effects resulting merely from the different crystal packing observed between solvent-free **1g** and **1g**·C_6D_6. The W-N-C bond angles fall in the range 171.5 - 178.6° and are similar for each dimeric imido derivative. The sum of the angles N-W-Cl(n) (n = 1 - 4) is the same for complexes **1f** and **g** (~391°), suggesting that the steric pressure of the imido ligand on the four Cl_n (n = 1 - 4) atoms, which displaces the tungsten center out of the Cl(1)-Cl(2)-Cl(3)-Cl(4) plane, is independent of the imido substituent.

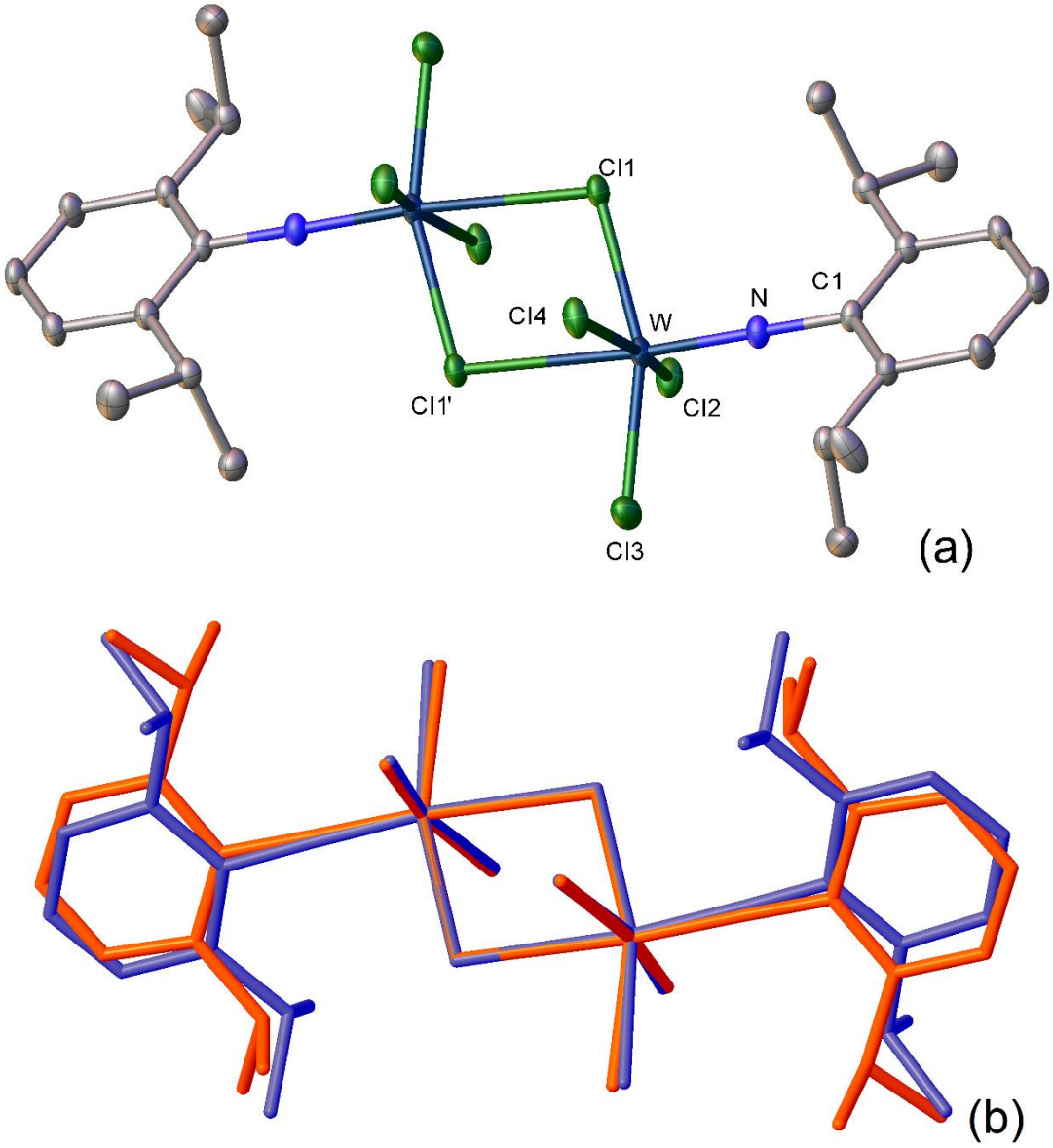

Figure 3. (a) X-ray molecular structure of [{WCl_3(μ-Cl)(NDipp)}$_2$] (**1g**) in the solvent-free crystal; (b) overlay of the structures of solvent-free **1g** (red) and **1g**·C_6D_6 (blue), omitting H atoms. The dihedral angle between the W_2Cl_2 and arene rings is 35.7° (**1g**) and 49.4° (**1g**·C_6D_6), respectively. Thermal ellipsoids are drawn at 50% probability level. Primed atoms are related by an inversion center.

The solid state structures of complexes **2f,g** have been determined by single crystal X-ray diffraction (Table 1, Figure 4) and found to be analogous (during the production of this manuscript

the structure of [WCl_4(NDipp)(thf)] (**2g**) was reported by O'Hare and co-workers at a different temperature; the molecular structures are near-identical[38]). The tungsten coordination is octahedral, although distorted by the strong repulsive effect of the *pseudo*-W≡N bond, which manifest as a displacement of the W atom from the equatorial Cl_4 plane towards the imido ligand by ~0.25 Å in both **2f** and **2g**; a similar effect is also observed for related [WCl_4(NR)(L)] complexes.[47] This similarity suggests that the steric pressure of the imido ligands is again essentially independent of the nature of the substituents R, something in agreement with the steric demands estimated using the percentage of buried volume approach (%V_{bur}, vide infra). In both **2f** and **2g** the THF coordinates in a position trans to the imido ligand. Despite the differences in electronic character between the two aryl imido substituents, the W–O bond distance is identical in both complexes. Similarly, in complexes **2f** and **2g** both the length (consistent with pseudo-triply-bonded imido ligands, LX_2 coordination) and the trans effect imposed by the W≡N bond are comparable.

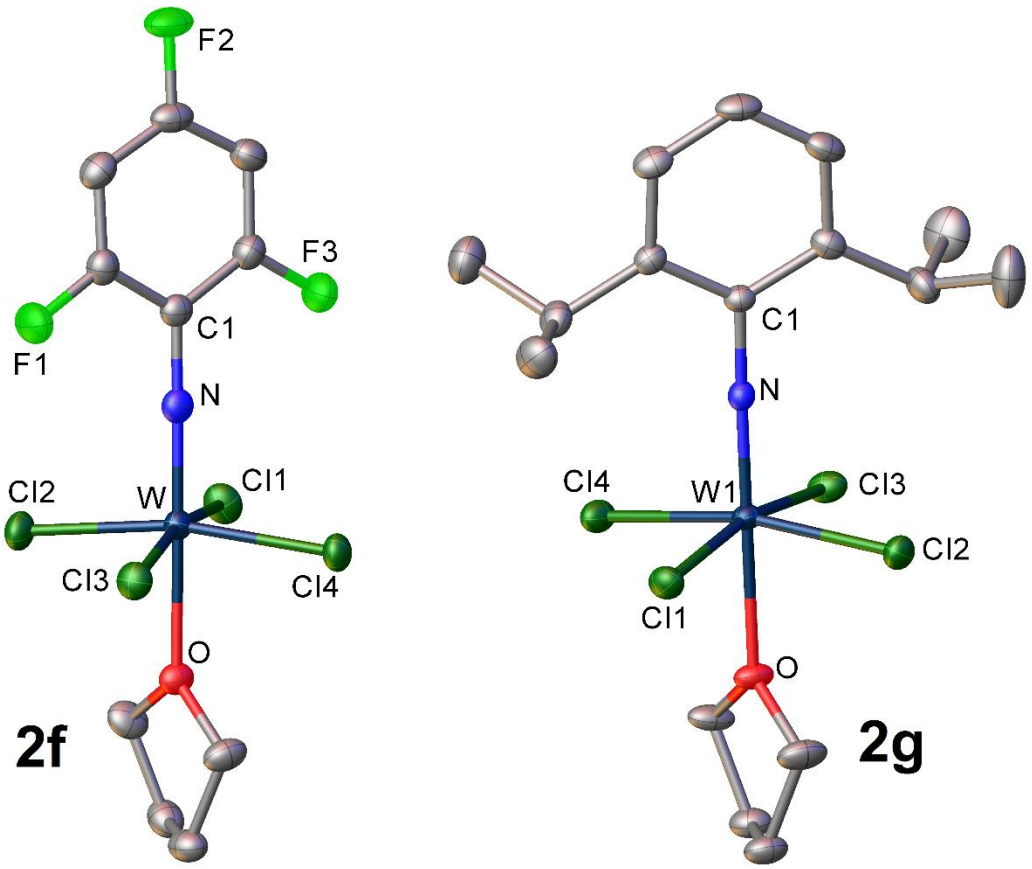

Figure 4. X-ray molecular structures of [WCl_4(NTfp)(thf)] (**2f**) and [WCl_4(NDipp)(thf)] (**2g**) showing one of the independent molecules. Thermal ellipsoids are drawn at 50% probability level.

1.2 Steric and Electronic Demands of the Imido Substituent. As demonstrated previously for both tungsten-based dimerization catalyst systems generated in situ and those employing discrete bis(imido) tungsten pre-catalysts, the characteristics of the organoimido ligand have a direct impact on catalytic performance.[24,35,37,38,39] Consequently, the steric and electronic nature of the various imido moieties used in the current study have been assessed and subsequently related to catalytic performance.

The steric demands of the organoimido ligands were probed using a combination of the ligand buried volume (%V_{Bur}, a molecular descriptor analogous to Tolman's cone angle) and topographic

steric map approaches (Table S5), as developed by Cavallo, Nolan, and co-workers.[61-65] In our study, although the THF adducts of complexes **2a-g** were used for catalysis testing (due to their greater solubility), their base-free halide-bridged dimers **1a-g** were selected for a comparative structural investigation due to the availability of a more extensive range of crystallographic data with which to make comparisons. This provides a self-consistent method for assessing the structural influences of the various organoimido moieties.

For the imido complexes **1a-g** (in each case the C-N-W bond angle is essentially 180°) the percentage volume (%V_{Bur}) occupied by the various ligands at the metal center varies as expected with the minimum observed for the ethyl imido complex **1a** and the maximum for 2,6-diisopropyl phenyl derivative **1g**; the values of %V_{Bur} span the range 17.3 – 23.8% (Table 2). Complexes bearing para-substituted imido ligands such as **1e** and its methyl analogue have almost identical values of %V_{Bur} consistent with substitution on the para position of the aryl imido having no steric impact on the metal center. Consideration of the corresponding topographic steric maps reveals that the various different imido motifs provide quite distinct steric environments about the tungsten center (e.g. **1g** vs **1e**, Table S6) with the NDipp motif locating substituents closest to the metal.

Table 2. Comparison of percent buried volume (%V_{Bur}),[61-65] W–N, W–Cl bond distances, and computed pK_a values of the parent aminium ions ($[H_3NR]^+$)[66] for assessing the steric and electronic demand of organoimido ligands (NR) of complexes **1a-c**,**e-g**.

Complex	**%V_{Bur} (NR)**	**W–N** (Å)	**W–Cl** (Å) [a]	**pK_a ($[H_3NR]^+$)**
[{WCl_3(μ-Cl)(NEt)}$_2$] (**1a**) [50]	17.4	1.69(1)	2.731(4)	10.6
[{WCl_3(μ-Cl)(N*i*Pr)}$_2$] (**1b**) [49]	18.6	1.697(8)	2.736(3)	10.6
[{WCl_3(μ-Cl)(N*c*Hx)}$_2$] (**1c**) [b]	--	--	--	10.6
[{WCl_3(μ-Cl)(N*t*Bu)}$_2$] [67]	20.0	1.704(5)	2.747(1)	10.7
[{WCl_3(μ-Cl)(NPh)}$_2$] (**1d**) [b]	--	--	--	4.6
[{WCl_3(μ-Cl)(N4-F-Ph)}$_2$] (**1e**) [59]	17.3	1.73(1)	2.709(4)	4.7
[{WCl_3(μ-Cl)(N4-Me-Ph)}$_2$] [60]	17.4	1.71(2)	2.718(7)	5.1
[{WCl_3(μ-Cl)(NTfp)}$_2$] (**1f**) [c]	19.2	1.7269(19)	2.6725(6)	1.9 [d]
[{WCl_3(μ-Cl)(NDipp)}$_2$] (**1g**) [c]	23.8	1.727(3)	2.7119(7)	4.3 [d]

[a] W–Cl bond distance for the fragment lying *trans* to the imido. [b] Molecular structure not determined. [c] This work. [d] Calculated using ACD/Labs software, version 11.02; ACD/Labs 1994-2016; the computational methodology employed herein has been independently validated.[68,69]

For the series of chloride-bridged dimers [{WCl_3(μ-Cl)(NR)}$_2$] (**1a-c**,**e-g**) there is minimal impact of the organic substituent R on the crystallographically-determined W–N_{imido} bond distances. The electron-rich alkyl-substituted imido ligands showed the shortest and the electron-withdrawing 2,4,6-trifluophenyl (Tfp) and 4-F-Ph derivatives the longest bonds, respectively (Table 2). Similarly, the range of W–Cl bond distances for the fragment lying trans to the imido in complexes **1a-c**,**e-g** is narrow, with the Tfp derivative **1f** having a shorter trans-W–Cl bond distance, indicative of a lower trans influence of this electron-poor organoimido moiety. Both sets of trends correlate with the corresponding pK_a values for the aminium ions of the parent amines confirming their electronic origins (Table 2).[50]

2. Dimerization catalysis testing. To probe the potential relationship between the well-defined mono(imido) pre-catalysts and those formed in situ from $WCl_6/ArNH_2/NEt_3$, catalytic tests were undertaken for each using identical conditions (Table 3 entries 1-7 and 8-11, respectively). Based on previous studies, a standard set of industrially relevant test conditions was used as a starting point, namely: $EtAlCl_2$ activator (W:Al 1:15), 40 barg ethylene pressure, 60 °C, and chlorobenzene (PhCl) solvent; these conditions match those used for the testing of related bis(imido) tungsten catalysts, enabling direct comparison.[24,35-39,76]

Table 3. Ethylene dimerization results at 40 barg ethylene pressure and 60 °C. [a]

Entry	Pre-catalyst	Time (min)	TON [b]	Activity[c]	Polymer product, wt%	C_4 in liq., wt% (1-C_4 in C_4, %)	C_6 in liq., wt% (1-C_6 in C_6, %)	Linear C_6 in C_6, %
1	$[WCl_4(NEt)(thf)]$ (**2a**)	3.9	1,700	25,840	1.2	79.4 (95.7)	19.6 (4.1)	6.5
2	$[WCl_4(N\textit{i}Pr)(thf)]$ (**2b**)	5.5	1,430	15,550	0.6	69.2 (95.1)	21.4 (3.5)	5.3
3	$[WCl_4(N\textit{c}Hx)(thf)]$ (**2c**)	3.5	2,120	36,340	2.6	53.9 (96.6)	46.1 (1.0)	36.8
4	$[WCl_4(NPh)(thf)]$ (**2d**)	12.9	27,110	125,957	0.2	73.7 (95.4)	17.8 (4.8)	11.1
5	$[WCl_4(N4\text{-}F\text{-}Ph)(thf)]$ (**2e**)	125.0	115,480	55,430	0.1	74.5 (97.5)	24.7 (3.3)	5.7
6	$[WCl_4(NTfp)(thf)]$ (**2f**)	94.0	124,730	79,720	0.0	73.1 (97.0)	22.1 (3.3)	4.3
7	$[WCl_4(NDipp)(thf)]$ (**2g**)	95.6	140,690	88,320	0.0	72.2 (98.0)	25.2 (1.5)	4.0
8	$WCl_6/PhNH_2/2\ NEt_3$ [d]	2.8	1,190	25,620	77.4	86.9	13.1	21.6

						(96.0)	(15.8)	
9	WCl_6/$DippNH_2$/2 NEt_3 [d]	2.5	902	21,660	96.3	94.8 (96.5)	5.2 (0.0)	0.0
10	WCl_6/2 $PhNH_2$/4 NEt_3 [d]	3.3	1,500	27,070	85.4	90.4 (97.3)	9.6 (19.5)	19.5
11	WCl_6/2 $DippNH_2$/4NEt_3 [d]	2.6	1,480	34,170	96.3	93.2 (100.0)	6.8 (0.0)	0.0
12	[WCl_4(NDipp)(thf)] (**2g**) [e]	16.1	3,820	14,250	0.8	67.6 (96.8)	31.9 (0.5)	5.4

[a] General conditions: 20 μmol W complex; 300 μmol $EtAlCl_2$ (15 eq to W); PhCl (solvent) 74 mL; 60 °C; ethylene pressure (40 barg); stirrer speed 1000 rpm; nonane standard (1.000 mL); catalytic runs were performed until consumption of C_2H_4 dropped below 0.2 g min^{-1} or until the reactor was filled. [b] TON (productivity) is reported in (mol C_2H_4)(mol W)$^{-1}$. [c] Activity is reported in (mol C_2H_4)(mol W)$^{-1}$ h^{-1}. [d] Pre-catalyst generated *in situ* using an analogous method to that reported previously with the molar ratios indicated in the table.[25] [e] Reaction stopped at low productivity.

2.1 Impact of Imido Substituent on Catalytic Activity and Productivity. Under identical test conditions the well-defined alkyl imido pre-catalysts (**2a-c**) gave activities that were lower than those of either their aryl imido-substituted analogues (**2d-g**) or the 'in situ' (WCl_6/$ArNH_2$/NEt_3) systems (Table 3, entries 1-11), but were approximately three orders of magnitude greater than the activities of the heterogeneous system reported by O'Hare and co-workers (MAO activator, 1 barg ethylene).[38,39] The catalytic lifetimes of both the 'in situ' and alkyl imido systems **2a-c** were comparable, but significantly shorter than those of the aryl imido derivatives, which lead to much lower productivities (at least one order of magnitude) for the former two systems (Table 3, entries 1-3 versus 4-7). In addition, whilst the rate of catalysis declined over time for all of the poorly performing pre-catalysts (Table 3, entries 1-4 and 8-11), for complexes **2e-g** the rate of catalysis increased over the course of reaction until the reaction vessel was filled with products (Table 3, entries 5-7; see SI for ethylene up-take traces).

In terms of catalytic performance, in contrast to the alkyl imido complexes, the aryl imido derivatives demonstrated clear trends that could be correlated with both the electronic and steric characteristics of the imido substituent (Figure 5). A comparison between the behavior of pre-catalyst complexes **2d** (NPh) and that of **2e** (N4-F-Ph) indicated that increasing the electron withdrawing nature of the imido substituent increased the catalyst lifetime five-fold (much higher productivity was achieved before the catalyst died), although activity was more than halved. A comparable trend has been reported previously for related systems.[24,39] Although pre-catalyst **2d** gave the most active system within this series, this is an artifact of its short catalytic lifetime (Figure S4). Examination of the behavior of pre-catalyst **2f**, bearing the yet more electron-withdrawing 2,4,6-trifluorphenyl (Tfp) imido substituent (Table 2), reveals a system that shows an enhancement in both activity and productivity relative to **2e**. However, tests performed with pre-catalyst **2g** possessing the sterically demanding and reasonably electron-donating 2,6-diisopropylphenyl (Dipp) substituent (Table 2) showed this system to be the most active and productive. This is consistent with steric factors dominating over electronic influences.

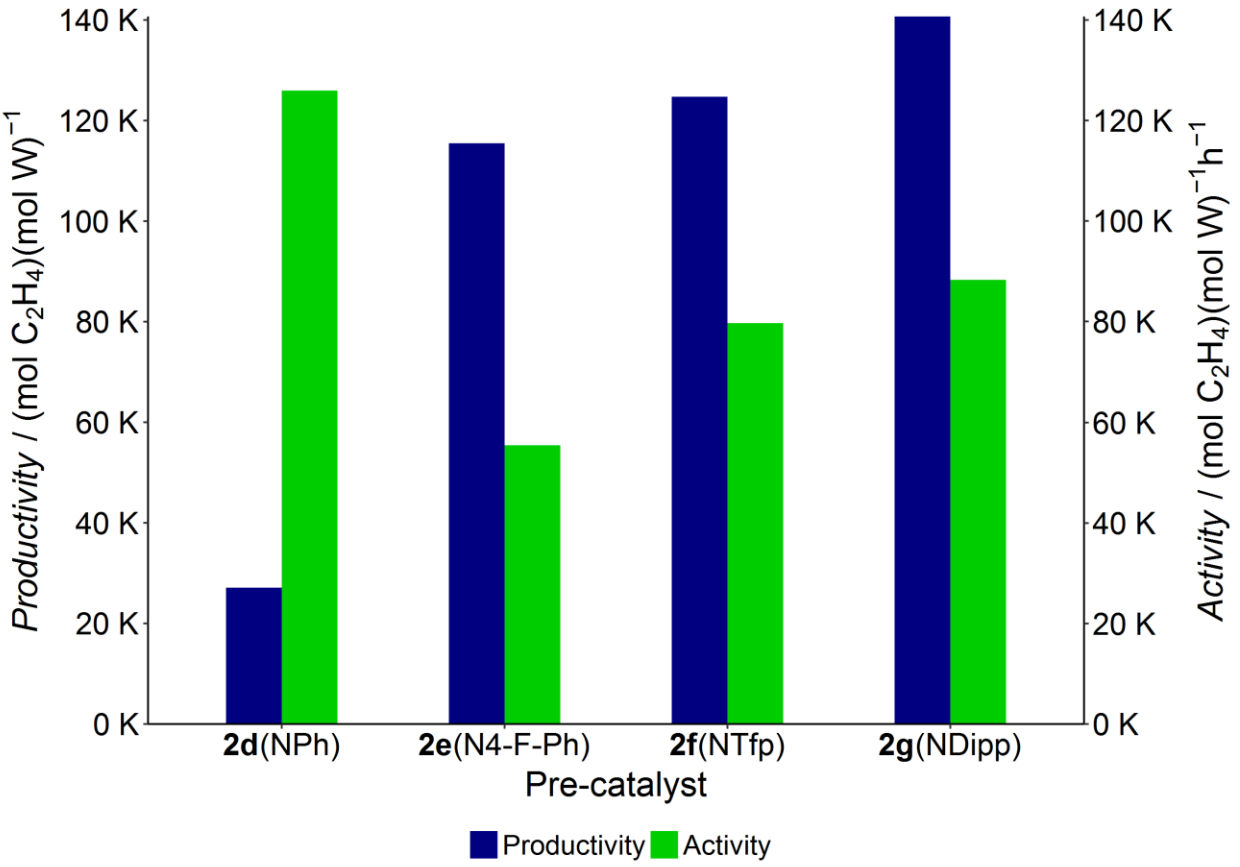

Figure 5. Activities and productivities achieved in the dimerization of ethylene at 60 °C and 40 barg using pre-catalysts **2d-g** (Table 3, entries 4-7).

2.2 Impact of Imido Substituent on Product Selectivity. From the data described above catalysts generated *in situ* from $WCl_6/ArNH_2/NEt_3$ (Table 3, entries 8-11) demonstrated both lower activities and productivities compared to those achieved when using pre-formed aryl imido complexes. Another clear distinction between these two classes of ethylene dimerization system lies in the level of polymer formation, with the in situ systems giving rise to product fractions comprising over 77 wt% polymer, whereas the well-defined imido-based pre-catalysts afforded little or no polymer (alkyl imido: 0.6 - 2.6 wt%; aryl imido: <0.1 wt%), Table 3, entries 8-11, 1-3, and 4-7. The low levels of polymer formation combined with the high productivity (vide supra) of

the well-defined aryl imido pre-catalysts make them strong candidates for applications on the industrial scale.

In terms of the liquid product fractions produced (Figure 6), all of the mono(imido) pre-catalysts yield butenes as the major product (53.9 wt% - 73.7 wt%), with high selectivities to 1-butene in the range 95.1% - 98.0%. For **2a**-**g** the selectivities to 1-hexene are very low within the C_6 (1.0 – 4.1%) fraction, which indicates that these C_6 materials form from incorporation of previously produced 1-butene rather than from direct trimerization of ethylene. This is consistent with the major byproducts resulting from product incorporation being branched in nature, specifically 2-ethyl-1-butene and 3-methyl-1-pentene, which are obtained in a roughly equal ratio here (Table S2).[70]

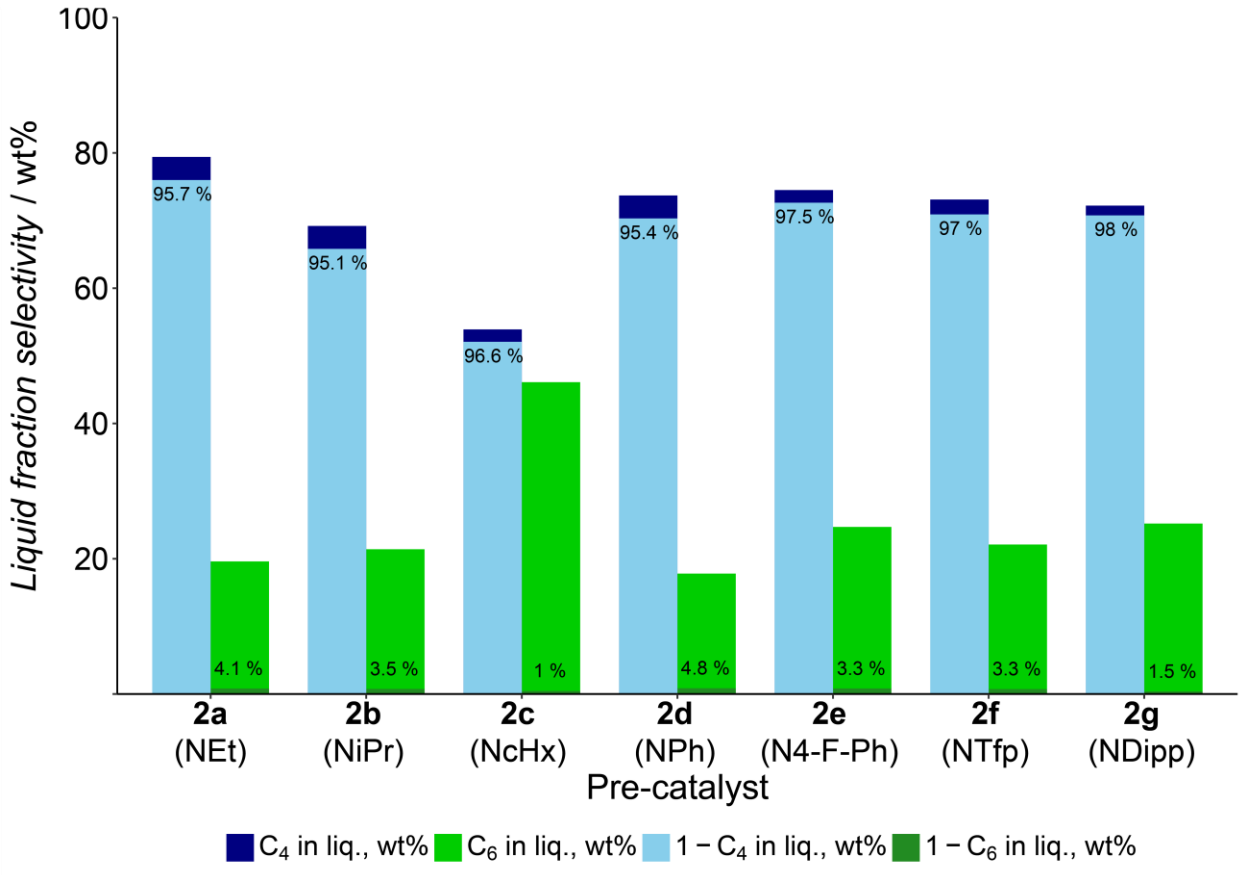

Figure 6. Product selectivities (wt%) towards butenes, 1-butene, hexenes (including methyl pentenes), and 1-hexene within the liquid fraction obtained from the dimerization of ethylene using pre-catalysts **2a-g** at 60 °C and 40 barg (Table 3, entries 1-7). Percentages given within the plot express the percentage of terminal linear alkene present within the C_4 and C_6 fractions.

For the alkyl imido-substituted pre-catalysts **2a-c** the nature of the imido substituent has no impact on the selectivity to 1-butene within the C_4 fraction, although an increase in bulk of the substituent at nitrogen (**2a** to **2c**) decreased selectivity to C_4, mainly as a result of increased C_6 formation. Comparing pre-catalysts **2d**-**g** (Figure 6), changing the nature of the aryl imido substituent has little effect on the liquid fraction selectivity, in particular, the overall amount of 1-butene produced is near-constant. Notably, despite pre-catalysts **2d** and **2g** (Table 3, entries 4 and 7, respectively) operating to significantly differing productivities, the extent of formation of C_{6+} byproducts is near identical. This demonstrates that the standing concentration of the primary product (1-butene) during catalysis does not influence C_{6+} production, something that is unusual as the amount of secondary incorporation products formed is usually proportional to the concentration of primary products.[71]

To explore the origins of the lack of impact of the standing concentration of 1-butene further, the test using [WCl_4(NDipp)(thf)] (**2g**)/$EtAlCl_2$ (entry 7 of Table 3) was repeated, but this time catalysis stopped after only 2.5 g of ethylene had been converted (by closing the supply of ethylene and cooling the reactor to –5 °C). This resulted in a decrease in the selectivity to the C_4 fraction, coupled with an increase in the proportion of the C_6 products compared with that determined for the equivalent reaction at much higher productivity (Table 3, entry 7). This confirms that for the tungsten mono(imido)-based catalysts described herein, the formation of C_6 and heavier products is indeed independent of the concentration of 1-butene. In addition, as described above, analysis

of the C_6 fraction shows that direct trimerization only occurs at very low levels, with the majority of the C_6 products being formed as a result of 1-butene incorporation (Scheme 4, Pathway 1). Taken together these results are consistent with either: a) 1-butene only being incorporated into heavy products when it has not been liberated from the catalytically active tungsten metal center (Scheme 4, Pathway 1); or b) that there is a secondary catalytic pathway in operation that is responsible for C_{6+} formation, which has a slower rate and is also independent of the amount of butene present (Pathway 2). These mechanistic proposals are consistent with the pathway through which the well-established ethylene trimerization system derived from Cr^{III}/2,5-dimthylpyrrole/Et_2AlCl unavoidably generates decenes, namely through immediate reaction of the newly formed Cr-hexene complex with ethylene.[70]

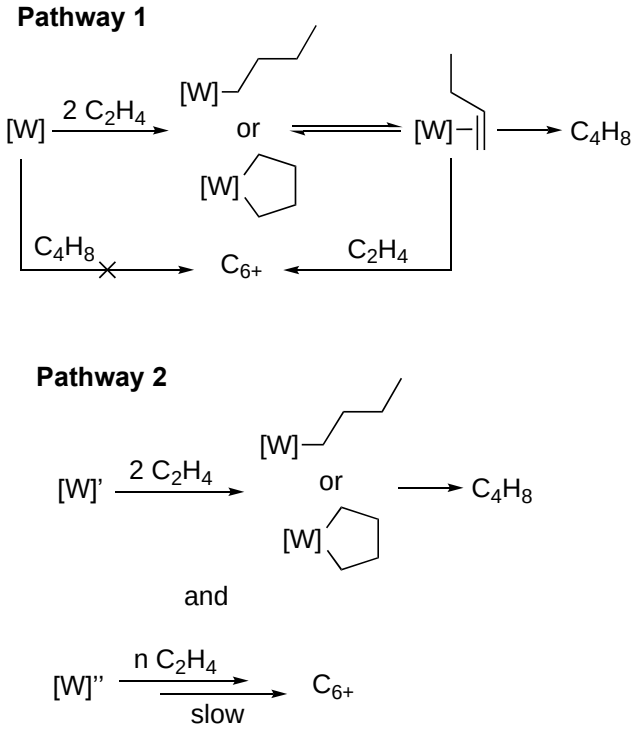

Scheme 4. Potential pathways for the formation of C_6 products mediated by mono(imido) tungsten pre-catalysts.

2.3 Temperature Effects on Catalysis. While test runs undertaken at 24 °C (Table 4, entries 6 and 7) gave no catalysis, raising the reaction temperature from 60 to 70 °C (and adjusting the ethylene pressure to maintain the same ethylene concentration in solution), led to an enhancement in catalytic performance, both in terms of activity and productivity (Figure 7 vs Figure 5).[72] The performance of the alkyl imido pre-catalyst **2c** was the outlier, having given a lower activity, but similar productivity compared to that obtained at 60 °C, with the amount of polymer produced also having increased (Table 4, entry 1). For tests at 70 °C the activity increased consistently through the series **2d-g**, although **2d** showed the same catalyst lifetime as the other pre-catalysts, in contrast to its weaker performance at 60 °C (see Figure 5 and Figure 7). Unlike the pronounced effect of increased temperature on activity and productivity, the selectivity of the aryl imido pre-catalysts was improved only slightly (up to 8.5 %), with **2e** being the most selective to 1-butene at both temperatures. Nevertheless, the liquid fraction selectivity to butenes for the alkyl imido pre-catalyst **2c** increased from 53.9 wt% to 77.1 wt%. This further highlights the significantly different catalytic behavior of aryl- compared with alkyl-imido pre-catalysts.

For catalytic tests undertaken at temperatures above 70 °C, controlling reaction exotherms became difficult. This meant that these tests were no longer isothermal across their duration and thus comparison of catalytic performance could not be made. Consequently, no catalytic tests at temperatures above 70 °C are reported here.

Table 4. Ethylene dimerization results at 45 barg ethylene pressure and 70 °C or at 9 barg ethylene pressure and 24 °C.[a]

Entry	Pre-catalyst	Time (min)	TON[b]	Activity[c]	Polymer product, wt%	C_4 in liq., wt% (1-C_4 in C_4, %)	C_6 in liq., wt% (1-C_6 in C_6, %)	Linear C_6 in C_6, %
1	[WCl_4(N*c*Hx)(thf)] (**2c**)	13.3	2,690	12,132	6.9	77.1 (93.9)	11.9 (4.8)	7.5
2	[WCl_4(NPh)(thf)] (**2d**)	53.6	144,290	161,410	0.0	81.2 (96.9)	17.1 (2.7)	4.2
3	[WCl_4(N-4-F-Ph)(thf)] (**2e**)	46.2	142,680	185,350	0.0	81.8 (96.9)	15.6 (3.0)	4.8
4	[WCl_4(NTfp)(thf)] (**2f**)	30.8	122,630	238,670	0.0	76.4 (97.0)	17.4 (3.8)	5.2
5	[WCl_4(NDipp)(thf)] (**2g**)	35.0	139,380	239,230	0.0	70.8 (97.9)	27.2 (1.6)	4.1
6	[WCl_4(NPh)(thf)] (**2d**)[d]	4.0	0	0	--	--	--	--
7	[WCl_4(NDipp)(thf)] (**2g**)[d]	10.0	0	0	--	--	--	--

[a] General conditions: 20 μmol W complex; 300 μmol $EtAlCl_2$ (15 eq to W); PhCl (solvent) 74 mL; 70 °C; ethylene pressure (45 barg); stirrer speed 1000 rpm; nonane standard (1.000 mL); catalytic runs were performed until consumption of C_2H_4 dropped below 0.2 g min^{-1} or until the reactor was filled. [b] TON (productivity) is reported in (mol C_2H_4)(mol W)$^{-1}$. [c] Activity is reported in (mol C_2H_4)(mol W)$^{-1}$ h^{-1}. [d] 24 °C; ethylene pressure (9 barg).

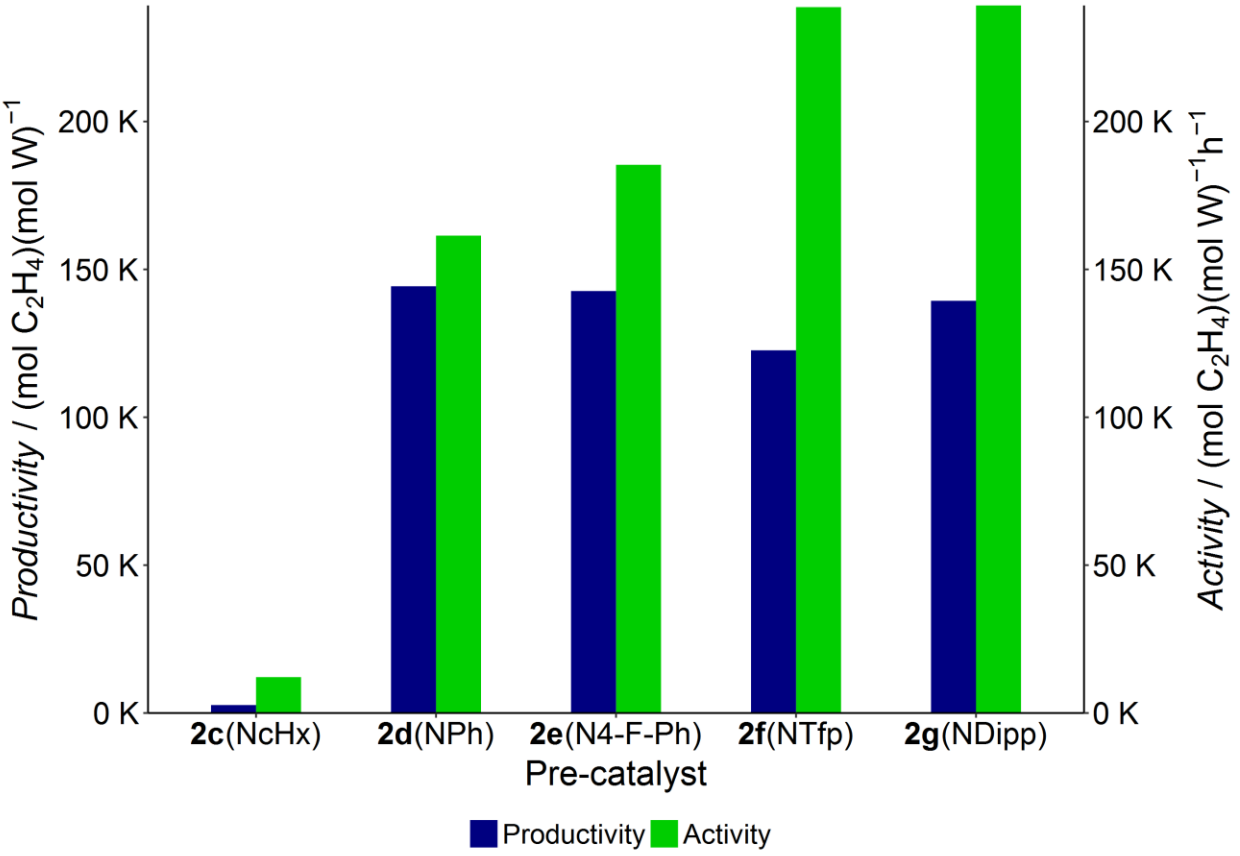

Figure 7. Activities and productivities achieved in the dimerization of ethylene at 70 °C and 45 barg using pre-catalysts **2c-g** (Table 4, entries 1-5).

2.4 Effect of the Aluminum Activator on Catalysis. It has been noted previously that the nature of the aluminum activator has a direct impact upon the catalytic performance of the 'in situ' tungsten/amine/base dimerization systems.[24,35,36] We have also observed similar behavior here for the discrete imido complexes **2d** and **2g** (Table 3, entries 4, 7 versus Table 5, entries 1, 2), with a marked decrease in the catalyst lifetime and activity being found with both pre-catalysts upon replacing $EtAlCl_2$ by $MeAlCl_2$. In contrast, the extent of polymer formation was identical with both the methyl and ethyl activators, i.e. trace levels. Although the selectivity within the liquid fraction remained broadly similar on replacing $EtAlCl_2$ for $MeAlCl_2$ with **2d**, the same change with **2g** lead to an increase in C_4 content from 72.2 wt% to 90.4 wt% accompanied by a decrease

in the selectivity to 1-butene by 17.2% and an increase in selectivity to 1-hexene of 21.1%. These effects reflect the nature of the mechanism through which the active catalyst is generated following Al-to-W transmetallation, a process in which the nature of the alkyl group will have a significant impact depending on whether this opens access to a β-H elimination pathway and hence the potential for a tungsten hydride-mediated catalytic cycle.[37]

Table 5. Ethylene dimerization results under varying reaction conditions. [a]

Entry	Pre-catalyst, *Activator (eq. to W)*	Time (min)	TON[b]	Activity[c]	Polymer product, wt%	C_4 in liq., wt% (1-C_4 in C_4, %)	C_6 in liq., wt% (1-C_6 in C_6, %)
1	[WCl_4(NPh)(thf)] (**2d**) *$MeAlCl_2$ (15)* [d]	2.8	2,028	43,980	0.5	77.6 (96.1)	21.7 (4.1)
2	[WCl_4(NDipp)(thf)] (**2g**) *$MeAlCl_2$ (15)* [d]	24.3	15,320	37,900	0.0	90.4 (80.8)	9.3 (22.6)
3	[{WCl_3(μ-Cl)(NDipp)}$_2$] (**1g**) *$EtAlCl_2$ (15)* [e]	71.7	21,330	17,860	0.0	62.8 (95.2)	13.9 (11.9)
4	[WCl_2(NPh)(PMe_3)$_3$] (**4a**) *$B(C_6F_5)_3$ (4)* [d]	18.3	0	0	--	--	--
5	[WCl(H)(NDipp)(PMe_3)$_3$] (**5**) *None*	5.6	0	0	--	--	--
6	[WCl(H)(NDipp)(PMe_3)$_3$] (**5**) *$AlCl_3$ (10)*	10.0	50	310	13.7	100 (96.3)	0.0
7	[WCl(H)(NDipp)(PMe_3)$_3$] (**5**) *$EtAlCl_2$ (15)*	19.6	4,320	13,250	0.0	97.5 (95.5)	2.5 (50.1)
8	[WCl_2(NPh)(PMe_3)$_3$] (**4a**) *$EtAlCl_2$ (15)* [d]	10.0	750	4,500	0.1	97.9 (98.1)	2.1 (100)
9	[WCl_2(NDipp)(PMe_3)$_3$] (**4b**) *$EtAlCl_2$ (15)* [d]	13.3	460	2,060	0.5	95.8 (100.0)	2.0 (100)
10	[{WCl_2(NDipp)}$_2$(μ-Cl)$_3$][Et_4N] (**3**) *$EtAlCl_2$ (15)* [e]	26.2	141,110	323,610	0.0	71.6 (98.1)	27.0 (1.6)

[a] General conditions: 20 μmol in W complex; PhCl (solvent) 74 mL; 70 °C; ethylene pressure 45 barg; stirrer speed 1000 rpm; nonane standard (1.000 mL); catalytic runs were performed until

consumption of C_2H_4 dropped below 0.2 g min^{-1} or until the reactor was filled. [b] TON (productivity) is reported in (mol C_2H_4)(mol W)$^{-1}$. [c] Activity is reported in (mol C_2H_4)(mol W)$^{-1}$ h^{-1}. [d] 60 °C; ethylene pressure 40 barg. [e] 10 μmol complex, therefore 20 μmol W, W:Al = 1:15.

2.5 Monomeric vs Dimeric Pre-Catalysts. Upon activation with $EtAlCl_2$ the dimeric complex [{WCl_3(μ-Cl)(NDipp)}$_2$] (**1g**) exhibited marked differences in catalytic performance compared to that of its analogous monometallic THF adduct **2g** under comparable test conditions (Table 4, entry 5 versus Table 5, entry 3). Note, however, that testing was undertaken with different concentrations of pre-catalyst (**1g** = 10 μmol; **2g** = 20 μmol) in order to keep the total amount of tungsten constant between the two runs; in both cases a W:Al ratio of 1:15 was maintained (300 μmol $EtAlCl_2$).

Although catalysis with complex **1g** was long-lived (71.7 min), this system demonstrated an activity that was over ten-fold lower compared to that achieved with **2g**, coupled with a significantly lower TON. In terms of selectivity **1g** was poor; although no polymer was generated the selectivity towards butenes was low (62.8 wt%) due to formation of C_{8+} products.

The poor catalytic performance of **1g** compared to that of **2g** is difficult to rationalize. The main differences between the two catalysis runs employing **1g** and **2g** are the lack of THF and the concentration of **1g** employed being half that of **2g** during activation, as a result of the dimeric nature of the former (note that both the total amount of tungsten and the concentration of $EtAlCl_2$ are the same in both runs). Both of these differences could alter significantly the activation process in each case, thus leading the observed differences in catalytic performance.

2.6 Effect of Tungsten Oxidation State. Given the possibility of W^{VI} reduction by $EtAlCl_2$ during catalysis (for example, *via* β-H elimination),[11] the catalytic behavior of W^{IV} mono(imido) derivatives (Table 5, entries 4-9) was compared with that of the W^{VI} precursors (**2d** and **2g**, Table

3, entries 4 and 7). Complex [$W^{IV}Cl_2(NPh)(PMe_3)_3$] (**4a**) was tested in the presence of four equivalents of $B(C_6F_5)_3$ to abstract the PMe_3 ligand to create a vacant coordination site for ethylene binding without changing the tungsten's oxidation state.[73] However, no ethylene uptake was observed (Table 5, entry 4). Consequently, considering the potential relevance of metal hydrides in ethylene dimerization reactions, a reaction using the complex [$W^{IV}Cl(H)(NDipp)(PMe_3)_3$] (**5**) was undertaken in the absence of $EtAlCl_2$ to explore whether the W-H moiety could initiate catalysis without the need for an additional activator (Table 5, entry 5).[3,74] However, no olefin uptake was observed in this case either. It must be noted that for the related bis(imido) catalyst systems both [$WCl_2(NDipp)_2(dme)$]/$EtAlCl_2$ and [$WCl_2(NDipp)_2(PMe_3)$]/$EtAlCl_2$ exhibit very similar ethylene dimerization performance, which indicates that the presence of PMe_3 cannot account for the differences between the mono(imido) W^{VI} and W^{IV} complexes examined herein.[76]

To enhance the reactivity of complex **5**, a test was conducted in which complex **5** was treated with 10 equivalents of $AlCl_3$ as a PMe_3 abstracting agent (Table 5, entry 6).[75] Under these conditions a very small amount of almost pure 1-butene was formed in the liquid fraction, but was accompanied by generation of ~14 wt% polymer. In contrast, activation of the W^{IV} complexes **4a**, **4b**, and **5** with $EtAlCl_2$ under standard reaction conditions afforded systems demonstrating only moderate performance (Table 5, entries 7-9) compared with that of the corresponding W^{VI} complexes (**2d** and **2g**, Table 3 entries 4 and 7; Table 4 entry 5). The productivities and activities of the W^{IV} pre-catalysts **4** and **5** in combination with $EtAlCl_2$ were at least 18 times lower than those observed using the corresponding W^{VI} pre-catalysts. In terms of selectivity, whilst the split between liquid and solid product fractions was very similar with both the W^{IV} and W^{VI} systems in combination with $EtAlCl_2$, the selectivity within the liquid fraction for the W^{IV} systems is much higher to C_4

products, such that the overall selectivity to 1-butene was >95 wt%, as expected at lower productivity.

A preliminary examination of the performance of tungsten(V) pre-catalysts was also undertaken. Thus, complex [{WCl_2(NDipp)}$_2$(μ-Cl)$_3$][Et_4N] (**3**) was tested in combination with $EtAlCl_2$ (W:Al 1:15) at 45 barg ethylene / 70 °C at a loading of **3** of 10 μmol (Table 5, entry 10). Under these conditions the W^V pre-catalyst **3** proved 35% more active for ethylene dimerization than the corresponding W^{VI} pre-catalyst **2g**, with both systems giving solely liquid products and almost identical selectivities within the liquid fraction (Table 5, entry 10 vs Table 4, entry 5).

Although W^{IV} mono(imido) pre-catalysts can afford active ethylene dimerization systems, based on the low activity observed they are unlikely to be the principle species generated upon activation of W^{VI} mono(imido) pre-catalysts with $EtAlCl_2$. In contrast, the higher productivity and identical selectivity achieved using the W^V mono(imido) pre-catalyst compared with that of its W^{VI} counterparts, tentatively suggests that W^V species are likely candidates for the true active species in these tungsten mono(imido)-based ethylene dimerization systems. However, a W^{IV} active catalyst cannot be completely excluded since it is possible that the sequence of activation reactions necessary to achieve the active catalyst may simply not be available to the selected W^{IV} pre-catalysts. Indeed, certainty about the oxidation state of the dimerization-active tungsten species can only be achieved following detailed kinetic analyses, something that is outside the scope of this preliminary study.[77]

2.7 Comparison with other ethylene dimerization systems. An important comparison required for any new ethylene dimerization catalyst system is its performance against that of Axens' AlphaButol process, employing $Ti(OBu)_4/Et_3Al$, which is currently the only commercialized

protocol.[23,24,79-81] Both AlphaButol and the tungsten mono(imido) pre-catalysts have demonstrated acceptable catalyst lifetimes (35 min for W, ~60 min for Ti), together with reasonable ethylene consumptions (78 g for W and 261 g for Ti); see Table S2. The best performing tungsten system described herein, **2d** ([WCl_4(NPh)(thf)]), outperforms the AlphaButol process (see Tables 3–5); **2d**: ~144,000 (mol C_2H_4)(mol W)$^{-1}$, moderate selectivity (~81%) for dimerization (selectivity to 1-butene ~97%) versus AlphaButol: ~16,550 (mol C_2H_4)(mol Ti)$^{-1}h^{-1}$, 1-butene selectivity ~95%. Notably, pre-catalyst **2d** does not generate polymeric products, which is a major advantage; despite early reports of trace polymer formation occurring with AlphaButol, later reports do however document examples free from polymer.[79-81] Comparison on a mass rather than on a mole basis, the activity of pre-catalyst **2d** (21,980 g(gW)$^{-1}h^{-1}$) is only around double that of AlphaButol (9,700 g(gTi)$^{-1}h^{-1}$) a benefit outweighed by the difference in cost of tungsten vs titanium. Nevertheless, it must be borne in mind that no optimization of the tungsten mono(imido) systems has been undertaken.

Further comparison of the performance of the tungsten mono(imido) pre-catalysts described here with other systems reported in the literature is challenging due to significant difference in test conditions employed. However, a brief assessment of the relative performance of the mono(imido) tungsten pre-catalysts described herein is informative.

One of the most active ethylene dimerization systems reported in the literature uses vanadium imido complex pre-catalysts activated with methylaluminoxane.[78] The activities reported reach an impressive 2,730,000 (mol C_2H_4)(mol V)$^{-1}$ h^{-1} with a productivity of 455,000 (mol C_2H_4)(mol V)$^{-1}$ and selectivity to 1-butene of 92.1%. However, the catalysis tests were performed for 10 minutes with only 6.37 g of ethylene being consumed, details that preclude making any assessment of industrially important catalyst lifetime.[78] As described above, in contrast, catalysis with **2g** with

(15 eq. $EtAlCl_2$, 70 °C) is sustained for 35 minutes and was only terminated when the reactor was filled with products (Table S2).

Notably, O'Hare and co-workers have also reported ethylene dimerization mediated by **2g** in combination with both soluble and polymer-immobilized MAO activators,[38] and have disclosed how catalytic performance (at 1 barg ethylene pressure) varies as a function of changes to the tungsten imido motif. The trends established mirror those we describe here in terms of the steric and electronic demands of the organoimido substituent.[39] However, the activities and productivities reported by O'Hare were <10 (mol C_2H_4)(mol W)$^{-1}$ and <100 (mol C_2H_4)(mol W)$^{-1}h^{-1}$, respectively. These values are around three orders of magnitude lower than those we describe herein, obtained at 70 °C, 45 barg ethylene, and with $EtAlCl_2$ as activator. This highlights the significant impact of catalyst test conditions. In particular, choice of aluminum activator can have a dramatic effect on performance. For example, we have demonstrated here that $EtAlCl_2$ outperforms its methyl analogue (Table 5; vide infra), a trend that was mirrored in the behavior of the in situ system disclosed previously, where MAO was also found to perform poorly.[35]

In terms of selectivity, the reports from O'Hare document impressive selectivities of >99% towards 1-butene achieved using the tungsten mono(imido) pre-catalysts such as **2g** (cf. ~97% 1-butene at 70 °C, 45 barg ethylene, and with $EtAlCl_2$).[38, 39] However, it must be noted that generally high selectivities are more easily achieved at lower productivities where the concentration of 1-butene is low, hence reducing the potential of 1-butene re-insertion.[76]

3.0 Reactivity of Tungsten Mono(Imido) Complexes.

As described above, the nature of the aluminum activator can have a profound impact on catalyst performance. Consequently, to gain further mechanistic insight into the tungsten mono(imido)-catalyzed dimerization of ethylene, in particular the role of the aluminum activator, an investigation of the reactivity of tungsten mono(imido) complexes and various alkylaluminum reagents in vitro was undertaken.

3.1 Reactions of [{WCl_3(μ-Cl)(NDipp)}$_2$] (1g) and [WCl_4(NDipp)(THF)] (2g) with $EtAlCl_2$ and Et_3Al. To probe the underlying mode of activation and hence assess subsequent catalytic behavior of complexes **1g** and **2g** in combination with aluminum activators, C_6D_6 solutions of complexes **1g** and **2g** were treated with $EtAlCl_2$ or Et_3Al in sealed NMR tubes and the resulting solutions analyzed by NMR spectroscopy. Complete consumption of both starting tungsten complexes **1g** and **2g** took place, which was accompanied by the formation of ethane (^{1}H NMR δ 0.80 ppm in C_6D_6) and other unidentified products. The appearance of ethane is consistent with a β-hydride/reductive elimination sequence from a [$WCl_x(Et)_{4-x}$(NR)] (x = 0 - 2) species formed via W/Al transmetallation – a process previously demonstrated to be facile.[37] Treating the **2g**/$EtAlCl_2$ solution with ethylene (1 barg) lead to an exothermic reaction, which afforded a mixture of C_4 (73 wt%), C_6 (22 wt%), and C_8 (2 wt%) alkenes (identified by GC analysis) with a distribution comparable to those determined for both the in situ and discrete mono(imido) systems in combination with $EtAlCl_2$ and ethylene (Table 3).

3.2 Reaction of [{WCl_3(μ-Cl)(NDipp)}$_2$] (1g) and [WCl_4(NDipp)(THF)] (2g) with Me_3Al. Reactions of **1g** and **2g** with ethylaluminum reagents produce complex product mixtures, consistent with access to a number of pathways, including β-H elimination, being possible. So, to facilitate understanding, analogous reactions with methylaluminum reagents were utilized to eliminate competition from β-H elimination processes. It should be noted that despite this

simplification, use of $MeAlCl_2$ as activator under the standard catalysis test conditions used here with the mono(imido) pre-catalysts, affords dimerization-active systems that yield similar product distributions (Table 1, entries 4, 7 versus Table 5, entries 1, 2), albeit with lower activities.

Treating complex **2g** with one or more equivalents of Me_3Al in CH_2Cl_2, C_6D_6 or C_6D_5Cl results in quantitative formation of the previously reported trimethyl complex [WCl(Me)$_3$(NDipp)] (**6**), Scheme 5 (the phenylimido analogue **6b** can be similarly synthesized from [WCl_4(NPh)(thf)], see SI) as also described by O'Hare.[38] The reaction is accompanied by formation of $AlCl_xMe_{(x-3)}$ and $AlCl_xMe_{(x-3)}$·thf adducts as identified by ^{1}H NMR spectroscopy (Figure S32). Notably, even in the presence of 4 equivalents of Me_3Al, no further reaction of **6** was found to occur (even on heating at 60 °C for 1 h), something consistent with previous reports of the difficulty in accessing [WMe_4(NAr)].[38,45]

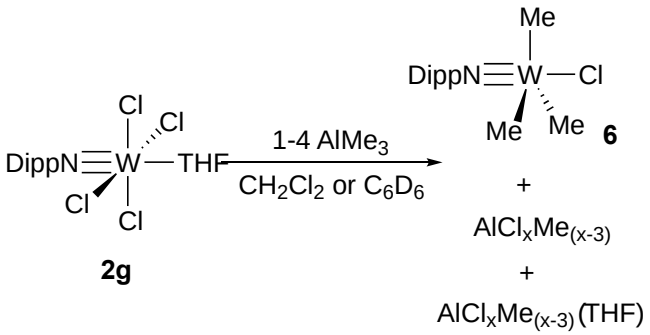

Scheme 5. Synthesis of [WCl(Me)$_3$(NDipp)] (**6**).

As was found with complex **2g**, reaction of the dimeric chloro-bridged complex [{WCl_3(μ-Cl)(NDipp)}$_2$] (**1g**) with two equivalents of Me_3Al (one equivalent per tungsten) again resulted in the methylation of the tungsten center, but this time the $AlCl_3$ adduct [WCl(Me)$_3$(NDipp)·$AlCl_3$] (**7**) was cleanly obtained and isolated, Scheme 6 (see SI for synthetic procedure). Complex **7** is analogous to the types of adduct formed in reactions between [WX(Np)$_3$(NMe)] (X = F, Cl, Br)

and ECl_3 (E = Al or Ga) reported previously by Osborn.[47] In solution the difference between complexes **6** and **7** is evident from their ^{1}H NMR spectra with the WMe_3 resonances appearing at 1.50 and at 1.43 ppm for complexes **7** and **6**, respectively, along with a broad aromatic resonance for **7** in place of the complex multiplets observed for **6** (Figure S33 and Figure S34). The ^{27}Al NMR spectrum of **7** is almost identical to that for the salt $[Et_3NH][AlCl_4]$ with a resonance observed at 104 ppm characteristic of discrete $AlCl_4$ anions (Figure S36), which is consistent with complex **7** having increased ionic character in solution and thus better represented as $[W(Me)_3(NDipp)][AlCl_4]$.[82] The increased ionic character of **7** is also demonstrated in the solid state (Figure S42) where the Al-Cl(1) bond (2.2253(6) Å) is longer than the mean Al-Cl bond in a discrete $AlCl_4$ anion (2.134(1) Å) by only 0.09 Å, a small elongation compared to the one observed for the W-Cl bond of **6** upon coordination with $AlCl_3$ (0.24 Å), consistent with a weak W···Cl-Al interaction and a strong $AlCl_4^-$ character.[83] Addition of THF, Et_4NCl, or excess Me_3Al to the $AlCl_3$-containing complex **7** results in the formation of the aluminum-free complex **6** (Scheme 6). This reactivity can be attributed to displacement of $AlCl_3$ through formation of $Cl_3Al(thf)_x$[84-85] or $AlCl_4^-$. However, it could also result from the presence of a high concentration of Me_3Al, which by alkylating the coordinated $AlCl_3$ leads to formation of a mixture of Me_2AlCl and Me_3Al, both of which are insufficiently Lewis acidic to strongly interact with the W-Cl motif (Figure S33). Note, that this weak association of the chloroaluminium species in **7**, resulting from Al-to-W transmetallation, contrasts with the products generated in vitro on reaction of $MeAlCl_2$ and bis(imido) complexes $[WCl_2(NAr)_2L_2]$ and also to computational predictions (e.g. **B**, Figure 1), which both show retention of alkylchloroaluminium species within the coordination sphere of tungsten via N_{imido}→Al coordination.[37] Lastly, it must be mentioned that no reaction occurred

when C_6D_6 or C_6D_5Cl solutions of **6** and **7** in isolation were treated with 1 barg ethylene in an NMR tube according to the ^1H NMR spectroscopic analysis.

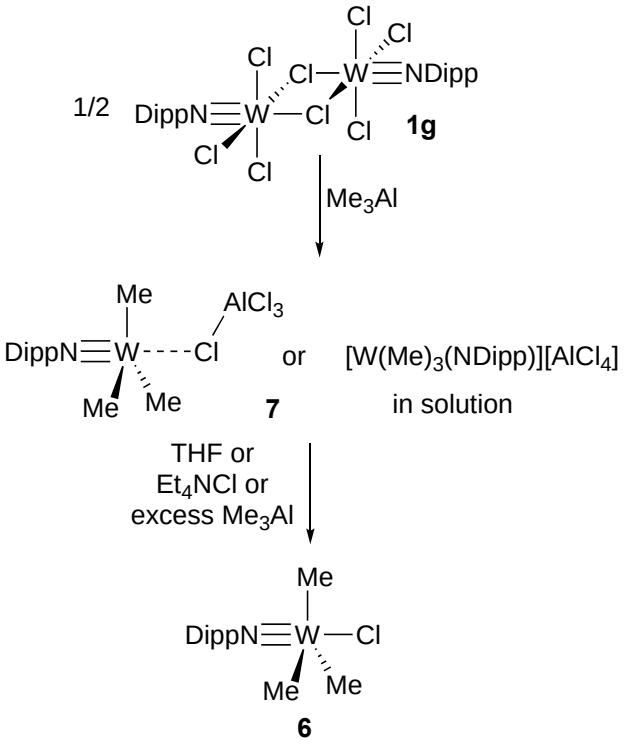

Scheme 6. Synthesis and reactivity of $[WCl(Me)_3(NDipp)\cdot AlCl_3]$ (**7**).

Together these results demonstrate that the primary initial role of the aluminum activator in the catalytic reactions described above is to alkylate the tungsten center and that formation of adducts between tungsten imido complexes and aluminum compounds is difficult in the presence of THF and/or large amounts of relatively weakly Lewis acid trialkylaluminums. Considering that formation of aluminum adducts of the various tungsten imido species is potentially key to obtaining active ethylene dimerization systems,[40-42] the observed inability of Me_3Al to form adducts with complex **6** is likely to explain why the variation in Lewis acid strength across the series R_xAlCl_{3-x} activators has such a pronounced effect on the catalytic performance of a given dimerization system. For instance, $EtAlCl_2$ is a better activator than ethylaluminum sesquichloride

(low productivity), while Et_3Al does not generate a catalytically active species at all in the *in situ* WCl_6/2 RNH_2/4 Et_3N system.[35] Furthermore, these observations are in accord with the report that ethylene dimerization mediated by **6**/MAO requires temperatures of 100 °C under 1 barg ethylene.[38]

3.3 Reaction of [{WCl_3(μ-Cl)(NDipp)}$_2$] (1g) and [WCl_4(NDipp)(THF)] (2g) with $MeAlCl_2$. In contrast to the reactions of **1g** and **2g** with Me_3Al, analogous reactions with the more catalytically relevant $MeAlCl_2$, results in a mixture of products, including methane and ethylene (Figures S37 and S38).[35] Although the fate of the tungsten imido fragments remains unknown for the reaction of **1g** with $MeAlCl_2$, the previously reported insoluble W^V imido complex **8** (identified by X-ray crystallography),[86] was isolated from the reaction with **2g** (Scheme 7).

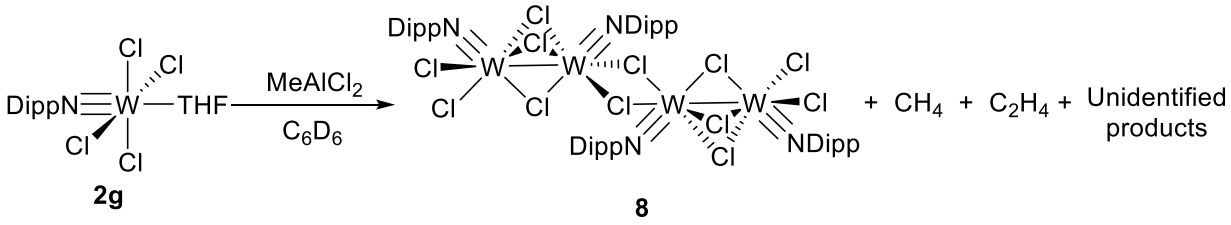

Scheme 7. Reaction of [WCl_4(NDipp)(thf)] (**2g**) with $MeAlCl_2$ to afford CH_4, C_2H_4, and **8**.

Formation of complex **8** demonstrates that generation of halide-bridged multimetallic W^V species akin to **3** is possible during catalysis. This, in combination with the high catalytic activity of **3**/$EtAlCl_2$ (Table 5, entry 10), further supports the notion that W^V is a likely oxidation state for tungsten in these mono(imido)-based tungsten dimerization catalysts. However, given that the most effective catalysts are generated using $EtAlCl_2$ rather than $MeAlCl_2$, the pathway through which a potential W^V active species is generated from a mono(metallic) W^{VI} starting material is less obvious, since the most likely reduction pathway is via Al-to-W ethyl transmetallation followed by reductive elimination, which would result in a 2 e^- reduction. Therefore, in order to

probe whether a pathway by which W^{V} complexes may be generated from W^{VI} during catalysis without passing through a dimeric species (such as described in Scheme 7) is viable, a CD_2Cl_2 solution of the W^{VI} complex [{WCl_3(μ-Cl)(NDipp)}$_2$] (**1g**) was treated with two equivalents of the W^{IV} derivative [WCl_2(NDipp)(PMe_3)$_3$] (**4b**). This resulted in the formation of the previously reported paramagnetic W^{V} complex [WCl_3(NDipp)(PMe_3)$_2$] (**9**),[51] as identified here by X-ray crystallographic analysis. The formation of **9** from **1g** and **4b** indicated that W^{V} species can be accessed via comproportionation of W^{VI} and W^{IV} species, which is again consistent with W^{IV} being unlikely to be involved in catalysis since it can be scavenged by the remaining W^{VI} resulting in the formation of W^{V} at the beginning of the reaction.

CONCLUDING REMARKS

In summary, a range of W^{VI} mono(imido) complexes were synthesized and found to be effective pre-catalysts for the dimerization of ethylene once activated with an appropriate alkylaluminum reagent. These systems gave selectivities towards 1-butene of up to 81.8 wt% and a maximum productivity of 139,380 (mol C_2H_4)(mol W)$^{-1}$ demonstrating their potential industrial relevance. Within the W^{VI} series, aryl imido catalysts performed better than their alkyl imido counterparts, especially when the aryl organomido substituents were bulky or electron withdrawing. In a preliminary manner, the oxidation state of the active catalyst during dimerization was probed by synthesizing and testing W^{V}, and W^{IV} mono(imido) complexes under various conditions. The tungsten(V) species were found to be over an order of magnitude more active and productive than the W^{IV}-derived systems, as well as 35% more active than the original W^{VI} complexes, consistent with W^{V} being the likely oxidation state during catalysis. Reactions of mono(imido) complexes with alkylaluminum reagents pointed towards a mechanism where the role of the aluminum activator is to first sequester any Lewis basic ligands (such as thf) present, then to alkylate the

tungsten(imido) complex. The resulting tungsten alkyl species then undergo by β-hydride elimination (in the case of $EtAlCl_2$) or hydride abstraction (for $MeAlCl_2$) accounting for the observed formation of ethane and of ethylene and methane, respectively. Isolation of W^V complexes from such reactions further supports the involvement of W^V in catalysis, while the presence of bound $AlCl_3$ on the tungsten appears to be key in the generation of active dimerization systems. Lastly, it is clear that a non-classical oligomerization pathway is responsible for the formation of C_{6+} products, since the standing concentration of the primary product (1-butene) during catalysis does not influence their production, which is unusual as the amount of secondary incorporation products formed is usually proportional to the concentration of primary products.

ASSOCIATED CONTENT

Supporting Information

The Supporting Information is available free of charge *via* the Internet on the ACS Publications website at http://pubs.acs.org.

Full synthetic methods, characterization data, catalysis procedures, ethylene uptake data, and crystallographic data in CIF format.

Accession Codes

CCDC 791643, 1520117, 1520118, 1520150–1520154, 1524554 and 1524556 contain the supplementary crystallographic data for this paper. These data can be obtained free of charge via www.ccdc.cam.ac.uk/data_request/cif, or by emaildata_request@ccdc.cam.ac.uk, or by

contacting The Cambridge Crystallographic Data Centre, 12 Union Road, Cambridge CB2 1EZ, UK; fax: +44 1223 336033.

AUTHOR INFORMATION

Corresponding Authors

* p.w.dyer@durham.ac.uk.

* Martin.Hanton@tuv-sud.co.uk

ORCID

Philip W. Dyer: 0000-0001-6576-5619

Martin J. Hanton: 0000-0002-1026-9199

Andrei S. Batsanov: 0000-0002-4912-0981

Judith A. K. Howard: 0000-0002-1871-4349

Antonis M. Messinis: 0000-0002-6168-355X

Author Contributions

The manuscript was written through contributions of all authors. All authors have given approval to the final version of the manuscript.

Notes

The authors declare no competing financial interests.

ACKNOWLEDGMENTS

The authors would like to thank Sasol Group Technology, the EPSRC, and Durham University for funding and permission to publish this work. Dr David Smith of Sasol Group Technology is thanked for fruitful discussions.

ABBREVIATIONS

Dipp, 2,6-diisopropylphenyl; MPs, methylpentenes; Tfp, 2,4,6-trifluorophenyl; TON, turnover number (productivity).

REFERENCES

(1) Dixon, J. T.; Green, M. J.; Hess, F. M.; Morgan, D. H. Advances in Selective Ethylene Trimerisation - a Critical Overview. *J. Organomet. Chem.* **2004**, *689*, 3641-3668.

(2) McGuinness, D. S. Olefin Oligomerization *via* Metallacycles: Dimerization, Trimerization, Tetramerization, and Beyond. *Chem. Rev.* **2011**, *111*, 2321-2341.

(3) Agapie, T. Selective Ethylene Oligomerization: Recent Advances in Chromium Catalysis and Mechanistic Investigations. *Coord. Chem. Rev.* **2011**, *255*, 861-880.

(4) van Leeuwen, P. W. N. M.; Clément, N. D.; Tschan, M. J. L. New Processes for the Selective Production of 1-Octene. *Coord. Chem. Rev.* **2011**, *255*, 1499-1517.

(5) Morgan, M. China's "New Normal": Slower Growth but Strong Prospects. *IHS Chemical Bulletin* **2016**, *2*, 3-6.

(6) Bender, M. An Overview of Industrial Processes for the Production of Olefins – C_4 Hydrocarbons. *ChemBioEng Reviews* **2014**, *1*, 136-147.

(7) Lee, G. S.; McCain, J. H.; Bhasin, M. M. *Kent and Riegel's Handbook of Industrial Chemistry and Biotechnology*, Springer Science & Business Media: Boston, MA, 2007.

(8) Breuil, P.-A. R.; Magna, L.; Olivier-Bourbigou, H. Role of Homogeneous Catalysis in Oligomerization of Olefins: Focus on Selected Examples Based on Group 4 to Group 10 Transition Metal Complexes. *Catal. Lett.* **2015**, *145*, 173-192.

(9) Geilen, F. M.; Stochniol, G.; Peitz, S.; Schulte-Koerne, E. Butenes. *Ullmann's Encyclopedia of Industrial Chemistry* 2014, pp 1-13.

(10) Skupinska, J. Oligomerization of α-Olefins to Higher Oligomers. *Chem. Rev.* **1991**, *91*, 613-648.

(11) Speiser, F.; Braunstein, P.; Saussine, W. Catalytic Ethylene Dimerization and Oligomerization: Recent Developments with Nickel Complexes Containing P,N-chelating Ligands. *Acc. Chem. Res.* **2005**, *38*, 784-793.

(12) Pillai, S. M.; Ravindranathan, M.; Sivaram, S. Dimerization of Ethylene and Propylene Catalyzed by Transition-metal Complexes. *Chem. Rev.* **1986**, *86*, 353-399.

(13) Al-Jarallah, A. M.; Anabtawi, J. A.; Siddiqui, M. A. B.; Aitani, A. M.; Al-Sa'doun, A. W. Ethylene Dimerization and Oligomerization to Butene-1 and Linear α-Olefins: A Review of Catalytic Systems and Processes. *Catal. Today* **1992**, *14*, 1-121.

(14) Datta, S.; Fischer, M. B.; Wreford, S. S. bisButadiene[1,2-bis(dimethylphosphino)ethane]titanium(0) Olefin Dimerizations Catalyzed by Titanium and Zirconium Butadiene Complexes. *J. Organomet. Chem.* **1980**, *188*, 353-366.

(15) Schrock, R.; McLain, S.; Sancho, J. Tantalacyclopentane Complexes and Their Role in the Catalytic Dimerization of Olefins. In *Pure Appl. Chem.*, 1980; Vol. 52, p 729.

(16) Bogdanović, B.; Spliethoff, B.; Wilke, G. Dimerization of Propylene with Catalysts Exhibiting Activities Like Highly-Active Enzymes. *Angew. Chem. Int. Ed. Engl.* **1980**, *19*, 622-623.

(17) Small, B. L.; Marcucci, A. J. Iron Catalysts for the Head-to-Head Dimerization of α-Olefins and Mechanistic Implications for the Production of Linear α-Olefins. *Organometallics* **2001**, *20*, 5738-5744.

(18) Lee, D. W.; Yi, C. S. Chain-Selective and Regioselective Ethylene and Styrene Dimerization Reactions Catalyzed by a Well-Defined Cationic Ruthenium Hydride Complex: New Insights on the Styrene Dimerization Mechanism. *Organometallics* **2010**, *29*, 3413-3417.

(19) Brookhart, M.; Hauptman, E. Mechanism of Rhodium(III)-Catalyzed Methyl Acrylate Dimerization. *J. Am. Chem. Soc.* **1992**, *114*, 4437-4439.

(20) Bhalla, G.; Oxgaard, J.; Goddard, W. A.; Periana, R. A. Hydrovinylation of Olefins Catalyzed by an Iridium Complex *via* CH Activation. *Organometallics* **2005**, *24*, 5499-5502.

(21) Buchard, A.; Auffrant, A.; Klemps, C.; Vu-Do, L.; Boubekeur, L.; Goff, X. F. L.; Floch, P. L. Highly Efficient P-N Nickel(II) Complexes for the Dimerisation of Ethylene. *Chem. Commun.* **2007,** 1502-1504.

(22) Gilbert, B.; Olivier-Bourbigou, H.; Favre, F. Chloroaluminate Ionic Liquids: from their Structural Properties to their Applications in Process Intensification. *Oil & Gas Science and Technology - Rev. IFP* **2007**, *62*, 745-759.

(23) Grasset, F.; Magna, L. Method for Dimerization of Ethylene into Butene-1 Using a Composition Including a Titanium Complex and an Alkoxy Ligand Functionalised by a Heteroatom. IFP Energies Nouvelles, EP2388069 (A1), 2011.

(24) Olivier, H.; Laurent-Gerot, P. Homogeneous and Two-phase Dimerization of Olefins Catalyzed by Tungsten Complexes. The Role of Imido Ligands and Lewis Acids. *J. Mol. Catal. A: Chem.* **1999**, *148*, 43-48.

(25) Alt, H. G. Intelligent Catalysts for Ethylene Oligomerization and Polymerization. *Polyolefins Journal* **2015**, *2*, 17-25.

(26) Wideman, L. G. Preparation of 1-Butene. Goodyear Tire and Rubber Co, US Patent 3,813,453, 1974.

(27) Brown, M.; Menapace, H. R.; Maly, N. A. Olefin Dimerization Process. Goodyear Tire and Rubber Co, US Patent 3,897,512, 1975.

(28) Maly, N. A.; Menapace, R.; Benner, G. S. Dimerization or Codimerization of α-Olefins. Goodyear Tire and Rubber Co, US Patent 3,784,629, 1974.

(29) Maly, N. A.; Menapace, R.; Benner, G. S. Dimerization or Codimerization of α-Olefins. Goodyear Tire and Rubber Co, US Patent 3,784,630, 1974.

(30) Maly, N. A.; Menapace, R.; Benner, G. S. Dimerization and Codimerization of Olefins. Goodyear Tire and Rubber Co, US Patent 3,903,193, 1975.

(31) Menapace, R.; Benner, G. S.; Maly, N. A. Dimerization or Codimerization of α-Olefins. Goodyear Tire and Rubber Co, US Patent 3,784,631, 1974.

(32) Menapace, H. R.; Maly, N. A.; Wang, J. L.; Wideman, L. G. Changing Reaction Paths of a Metathesis Catalyst. *J. Org. Chem.* **1975**, *40*, 2983-2985.

(33) Hendriksen, D. E. Hydrogen chloride free catalyst system for dimerizing and codimerizing olefins. Exxon Chemicals Inc., US Patent 5,059,739, 1991.

(34) Wideman, L. G. Preparation of 1-Butene. Goodyear Tire and Rubber Co, US Patent 3,813,453, 1974.

(35) Hanton, M. J.; Daubney, L.; Lebl, T.; Polas, S.; Smith, D. M.; Willemse, A. Selective Dimerization of Alpha-Olefins Using Tungsten-Based Initiators. *Dalton Trans.* **2010**, *39*, 7025-7037.

(36) Tooze, R. P.; Hanton, M. J. Tungsten-based Catalyst System. SASOL Technology (UK) Limited, WO 2005/089940 A2, 2005.

(37) Wright, W. R. H.; Batsanov, A. S.; Howard, J. A. K.; Tooze, R. P.; Hanton, M. J.; Dyer, P. W. Exploring the Reactivity of Tungsten bis(Imido) Dimethyl Complexes with Methyl

Aluminium Reagents: Implications for Ethylene Dimerization. *Dalton Trans.* **2010**, *39*, 7038-7045.

(38) Wright, C. M. R.; Turner, Z. R.; Buffet, J.-C.; O'Hare, D. Tungsten Imido Catalysts for Selective Ethylene Dimerization. *Chem. Commun.* **2016**, *52*, 2850-2853.

(39) Wright, C. M. R.; Williams, T. J.; Turner, Z. R.; Buffet, J.-C.; O'Hare, D. Selective Ethylene Oligomerization Using Supported Tungsten mono-Imido Catalysts. *Inorg. Chem. Front.* **2017**, *4*, 1048-1060.

(40) Tobisch, S. alpha-Olefin Dimerization by a mono(Imido) Tungsten Catalyst: Computational Evidence for the Role of Lewis Acid Chelates in Effective Catalysis. *Organometallics* **2007**, *26*, 6529-6532.

(41) Tobisch, S. Stable Lewis Acid Chelate of a bis(Imido) Tungsten Compound and Implications for alpha-Olefin Dimerization Catalysis: a DFT Study. *Dalton Trans.* **2008**, 2120-2127.

(42) Tobisch, S. Tungsten Imido-catalysed Dimerization of α-Olefins: Insight into the Lewis Acid's Function Revealed from Computational Studies. *Procedia Computer Science* **2011**, *4*, 1203-1213.

(43) Ison, E. A.; Abboud, K. A.; Boncella, J. M. Synthesis and Reactivity of Molybdenum Imido Diamido Metallacyclopentenes and Metallacyclopentadienes and the Mechanism of Ethylene Exchange with Metallacyclopentane Complexes. *Organometallics* **2006**, *25*, 1557-1564.

(44) Gibson, V. C.; Kee, T. P.; Shaw, A. New, Improved Synthesis of the Group-6 Oxyhalides, $W(O)Cl_4$, $W(O)_2Cl_2$ and $MO(O)_2Cl_2$. *Polyhedron* **1988**, *7*, 579-580.

(45) Bradley, D. C.; Hursthouse, M. B.; Malik, K. M. A.; Nielson, A. J.; Short, R. L. Organoimido-Complexes of Tungsten-(VI) Tungsten-(V), and Tungsten-(IV) - Crystal and Molecular-Structures of $W(NPh)Cl_3(PPh_3)_2$ and $W(NPh)Cl_2(PMe_3)_3$. *J. Chem. Soc., Dalton Trans.* **1983**, 2651-2656.

(46) Schrock, R. R.; Depue, R. T.; Feldman, J.; Yap, K. B.; Yang, D. C.; Davis, W. M.; Park, L.; Dimare, M.; Schofield, M.; Anhaus, J.; Walborsky, E.; Evitt, E.; Kruger, C.; Betz, P. Further-Studies of Imido Alkylidene Complexes of Tungsten, Well-Characterized Olefin Metathesis Catalysts with Controllable Activity. *Organometallics* **1990**, *9*, 2262-2275.

(47) Leny, J. P.; Osborn, J. A. Synthesis and Study of Imidoalkyl Complexes of Tungsten(VI) - Application of N-14 NMR-Spectroscopy. *Organometallics* **1991**, *10*, 1546-1550.

(48) Bradley, D. C.; Errington, R. J.; Hursthouse, M. B.; Short, R. L.; Ashcroft, B. R.; Clark, G. R.; Nielson, A. J.; Rickard, C. E. F. Preparation and Characterization of Mononuclear Organoimido Complexes of Tungsten - X-Ray Crystal-Structures of $[WCl_4(NC_6H_4Me\text{-}para)(THF)]$,$[P(CH_2Ph)Ph_3]$-$[WCl_5(NC_6H_4Me\text{-}para)]$, and $[WCl_2(NPh)_2(BIPY)]$. *J. Chem. Soc., Dalton Trans.* **1987**, 2067-2075.

(49) Hayano, S.; Tsunogae, Y. Syndioselective Ring-Opening Metathesis Polymerization of endo-Dicyclopentadiene with Tungsten Complexes Having Imido Ligands: Development of Crystalline Syndiotactic Hydrogenated Poly(endo-dicyclopentadiene). *Macromolecules* **2006**, *39*, 30-38.

(50) Ashcroft, B. R.; Clark, G. R.; Nielson, A. J.; Rickard, C. E. F. Studies of π-Bonding Perturbation in the Tungsten-Nitrogen Multiple Bond of Isopropylimido Tungsten(VI) Complexes: The Crystal and Molecular Structures of $[W(NCHMe_2)Cl_4]_2 \cdot C_6H_6$ and $[W(NCHMe_2)Cl_5][NEt_4]$. *Polyhedron* **1986**, *5*, 2081-2091.

(51) Bradley, D. C.; Errington, R. J.; Hursthouse, M. B.; Short, R. L. Synthesis and Characterisation of Binuclear and Trinuclear Organoimido Complexes of Tungsten-(VI) and -(V) and a Binuclear Tungsten(V) Oxoanion. X-Ray Crystal Structures of $[\{WCl_4(NEt)\}_2]$, $[P(CH_2Ph)Ph_3][W_3Cl_7(NBu^t)_3(\mu\text{-}NPh)_3]$, $[P(CH_2Ph)Ph_3][W_2Cl_7(NR)_2]$(R = Et or Ph), and $[P(CH_2Ph)Ph_3][W_2O_2Cl_7]$. *J. Chem. Soc., Dalton Trans.* **1990**, 1043-1051.

(52) Clark, G. R.; Nielson, A. J.; Rickard, C. E. F. Evaluation of the 2,6-Diisopropylpheylimido Ligand as a Steric Force in d(1) and d(2) Monomeric Octahedral Complexes of Tungsten. *J. Chem. Soc., Dalton Trans.* **1995**, 1907-1914.

(53) Peterson, E.; Khalimon, A. Y.; Simionescu, R.; Kuzmina, L. G.; Howard, J. A. K.; Nikonov, G. I. Diversity of Catalysis by an Imido-Hydrido Complex of Molybdenum. Mechanism of Carbonyl Hydrosilylation and Silane Alcoholysis. *J. Am. Chem. Soc.* **2008**, *131*, 908-909.

(54) Collings, J. C.; Roscoe, K. P.; Thomas, R. L.; Batsanov, A. S.; Stimson, L. M.; Howard, J. A. K.; Marder, T. B. Arene-Perfluoroarene Interactions in Crystal Engineering. Part 3. Single-Crystal Structures of 1:1 Complexes of Octafluoronaphthalene with Fused-Ring Polyaromatic Hydrocarbons. *New J. Chem.* **2001**, *25*, 1410-1417.

(55) Collings, J. C.; Roscoe, K. P.; Robins, E. G.; Batsanov, A. S.; Stimson, L. M.; Howard, J. A. K.; Clark, S. J.; Marder, T. B. Arene-Perfluoroarene Interactions in Crystal Engineering 8: Structures of 1:1 Complexes of Hexafluorobenzene with Fused-Ring Polyaromatic Hydrocarbons. *New J. Chem.* **2002**, *26*, 1740-1746.

(56) Gibson, V. C. Dalton perspectives. Structural and Bonding Patterns in Tetrahedral and *pseudo*-Tetrahedral Transition-metal Complexes Containing π-Donor Ligands. *J. Chem. Soc., Dalton Trans.* **1994**, 1607-1618.

(57) Green, M. L. H. A New Approach to the Formal Classification of Covalent Compounds of the Elements. *J. Organomet. Chem.* **1995**, *500*, 127-148.

(58) Won, Y. S.; Kim, Y. S.; Anderson, T. J.; Reitfort, L. L.; Ghiviriga, I.; McElwee-White, L. Homogeneous Decomposition of Aryl- and Alkylimido Precursors for the Chemical Vapor Deposition of Tungsten Nitride: A Combined Density Functional Theory and Experimental Study. *J. Am. Chem. Soc.* **2006**, *128*, 13781-13788.

(59) Hursthouse, M. B.; Howes, A. J.; Bradley, D. C.; Runnacles, J. D. CCDC-253821 *CSD communication,* 2004.

(60) Clegg, W.; Errington, R. J. Structure of di-[μ]-chloro-bis[trichloro(p-tolylimino)tungsten(VI)], [{WCl_3(p-$CH_3C_6H_4N$)}$_2$(μ-$Cl)_2$]. *Acta Crystallogr., Sect. C* **1987**, *43*, 2223-2224.

(61) Poater, A.; Ragone, F.; Giudice, S.; Costabile, C.; Dorta, R.; Nolan, S. P.; Cavallo, L. Thermodynamics of N-Heterocyclic Carbene Dimerization: The Balance of Sterics and Electronics. *Organometallics* **2008**, *27*, 2679-2681.

(62) Poater, A.; Cosenza, B.; Correa, A.; Giudice, S.; Ragone, F.; Scarano, V.; Cavallo, L. SambVca: A Web Application for the Calculation of the Buried Volume of N-Heterocyclic Carbene Ligands. *Eur. J. Inorg. Chem.* **2009**, 1759-1766.

(63) Poater, A.; Ragone, F.; Mariz, R.; Dorta, R.; Cavallo, L. Comparing the Enantioselective Power of Steric and Electrostatic Effects in Transition-Metal-Catalyzed Asymmetric Synthesis. *Chem. Eur. J.* **2010**, *16*, 14348-14353.

(64) Falivene, L.; Credendino, R.; Poater, A.; Petta, A.; Serra, L.; Oliva, R.; Scarano, V.; Cavallo, L. SambVca 2. A Web Tool for Analyzing Catalytic Pockets with Topographic Steric Maps. *Organometallics* **2016**, *35*, 2286-2293.

(65) Clavier, H.; Nolan, S. P. Percent Buried Volume for Phosphine and N-heterocyclic Carbene Ligands: Steric Properties in Organometallic Chemistry. *Chem. Commun.* **2010**, *46*, 841-861.

(66) Dean, J. A. In *Lange's Handbook of Chemistry*, 15 ed.; McGraw-Hill, Inc., 1999.

(67) Stahl, K.; Weller, F.; Dehnicke, K.; Paetzold, P. Bis[(tert-butylnitren)tetrachlorowolfram] Synthese, IR-Spektrum und Kristallstruktur. *Z. Anorg. Allg. Chem.* **1986**, *534*, 93-99.

(68) Rossini, E.; Netz, R. R.; Knapp, E.-W. Computing pK_a Values in Different Solvents by Electrostatic Transformation. *J. Chem. Theory and Comput.* **2016**, *12*, 3360-3369.

(69) Nieto-Draghi, C.; Fayet, G.; Creton, B.; Rozanska, X.; Rotureau, P.; de Hemptinne, J.-C.; Ungerer, P.; Rousseau, B.; Adamo, C. A General Guidebook for the Theoretical Prediction

of Physicochemical Properties of Chemicals for Regulatory Purposes. *Chem. Rev.* **2015**, *115*, 13093-13164.

(70) Zilbershtein, T. M.; Kardash, V. A.; Suvorova, V. V.; Golovko, A. K. Decene Formation in Ethylene Trimerization Reaction Catalyzed by Cr–Pyrrole System. *App. Cat. A: General* **2014**, *475*, 371-378.

(71) Walsh, R.; Morgan, D. H.; Bollmann, A.; Dixon, J. T. Reaction Kinetics of an Ethylene Tetramerization Catalyst. *App. Cat. A: General* **2006**, *306*, 184-191.

(72) Dashti, A.; Mazloumi, S. H.; Akbari, A.; Ahadiyan, H. R.; Emami, A. R. Solubility of Ethene in n-Hexane and n-Heptane as Common Slurry-Phase Polymerization Solvents: Experimental Measurement and Modeling. *J. Chem. Eng. Data.* **2016**, *61*, 693-697. Calculations suggest that at 60 °C and 40 barg the concentration of ethylene in solution is 3.56M, whilst at 70 °C and 45 barg the concentration is 3.58M and 80 °C and 50 barg the concentration is 3.61M. See *"Solubility of Gases in Liquids"*, Fogg, P. G. T.; Gerrard, W. Wiley, Chichester, 1991, (ISBN 0 471 92925 5); Chapter 7; Section 7.3; pages 133-140 and references therein for data and details of calculations.

(73) Chen, Y.; Wu, G.; Bazan, G. C. Remote Activation of Nickel Catalysts for Ethylene Oligomerization. *Angew. Chem. Int. Ed.* **2005**, *44*, 1108-1112.

(74) Müller, U.; Keim, W.; Krüger, C.; Betz, P. [{$Ph_2PCH_2C(CF_3)_2O$}NiH(PCy_3)]: Support for a Nickel Hydride Mechanism in Ethene Oligomerization. *Angew. Chem. Int. Ed. Engl.* **1989**, *28*, 1011-1013.

(75) Burt, J.; Levason, W.; Light, M. E.; Reid, G. Phosphine Complexes of Aluminium(III) Halides - Preparation and Structural and Spectroscopic Systematics. *Dalton Trans.* **2014**, *43*, 14600-14611.

(76) Messinis, A. M.; Wright, W. R. H.; Batsanov, A. S.; Howard, J. A. K.; Dyer, P. W.; Hanton, M. J. bis(Imido) bis(Imido) Tungsten Complexes: Efficient Pre-catalysts for the Homogeneous Dimerization of Ethylene *ACS Catal.* **2018** under revision.

(77) Bedford, R. B. How Low Does Iron Go? Chasing the Active Species in Fe-Catalyzed Cross-Coupling Reactions. *Acc. Chem. Res.* **2015**, *48*, 1485-1493.

(78) Zhang, S.; Nomura, K. Highly Efficient Dimerization of Ethylene by (Imido)vanadium Complexes Containing (2-Anilidomethyl)pyridine Ligands: Notable Ligand Effect toward Activity and Selectivity. *J. Am. Chem. Soc.* **2010**, *132*, 4960-4965.

(79) Le Quan, N.; Cruypelinck, D.; Commereur, D.; Chauvin, Y.; Leger, G. Procède Amélioré de Synthèse du Butène-1 par Dimerisation de l'Ethylène. IFP Energies Nouvelles, FR 2552079 A1, 1985.

(80) Magna, L.; Olivier-Bourbigou, H. Catalytic Composition and Process for the Selective Dimerization of Ethylene to 1-Butene. IFP Energies Nouvelles, US/2016/002124 A1, 2016.

(81) Magna, L.; Olivier-Bourbigou, H. Process for the Selective Dimerization of Ethylene to 1-Butene. IFP Energies Nouvelles, US 9,499,455 B2, 2016.

(82) George, K.; Jura, M.; Levason, W.; Light, M. E.; Reid, G. Thio-, Seleno- and Telluro-Ether Complexes of Aluminium(III) Halides: Synthesis, Structures and Properties. *Dalton Trans.* **2014**, *43*, 3637-3648.

(83) Gálvez-Ruiz, J. C.; Guadarrama-Pérez, C.; Nöth, H.; Flores-Parra, A. Group 13 Complexes of 5-Methyl-1,3,5-dithiazinane. *Eur. J. Inorg. Chem.* **2004**, 601-611.

(84) Bryliakov, K. P.; Babushkin, D. E.; Talsi, E. P.; Voskoboynikov, A. Z.; Gritzo, H.; Schröder, L.; Damrau, H.-R. H.; Wieser, U.; Schaper, F.; Brintzinger, H. H. *ansa*-Titanocene Catalysts for α-Olefin Polymerization. Syntheses, Structures, and Reactions with Methylaluminoxane and Boron-Based Activators, *Organometallics* **2005**, *24*, 894-904.

(85) Means, N. C.; Means, C. M.; Bott, S. G.; Atwood, J. L. Interaction of Aluminum Trichloride with Tetrahydrofuran. Formation and Crystal Structure of Dichlorotetrakis(tetrahydrofuran)aluminum(1^+) Tetrachloroaluminate(1^-). *Inorg. Chem.* **1987**, *26*, 1466-1468.

(86) Tanahashi, H.; Ikeda, H.; Tsurugi, H.; Mashima, K. Synthesis and Characterization of Paramagnetic Tungsten Imido Complexes Bearing α-Diimine Ligands. *Inorg. Chem.* **2016**, *55*, 1446-1452.